LARGE-SCALE OSCILLATIONS OF THE GALAXY AND THE KINEMATICS OF THE SOLAR NEIGHBOURHOOD

KONRAD KUIJKEN[1] AND SCOTT TREMAINE[1,2]

[1] *Canadian Institute for Theoretical Astrophysics, McLennan Labs, University of Toronto, 60 St. George Street, Toronto, Ontario M5S 1A1, Canada.*
E-mail: kuijken@cita.utoronto.ca
E-mail: tremaine@cita.utoronto.ca

[2] *California Institute of Technology, Pasadena, California 91125, USA.*

Abstract. To a good first approximation the Galaxy is stationary and axisymmetric. However, many disk galaxies exhibit prominent large-scale deviations from axisymmetry, such as bars, warps, "grand design" spiral structure, elliptical distortions of the bulge and disk, and lopsided HI distributions. In addition, models of galaxy formation strongly suggest that the dark matter halos of galaxies are likely to be triaxial, and the potential from these components will inevitably distort the disk. Thus it is natural to look for evidence of large-scale oscillations (*i.e.* non-axisymmetric distortions or axisymmetric time-dependent distortions) of the Galactic disk. Because of our location within the Galaxy, the large-scale kinematic models that we deduce for the Galaxy depend strongly on our interpretation of the small-scale kinematics of the solar neighbourhood. For example, asymmetry of the northern and southern HI distributions in velocity-longitude space could be caused by either a distortion of the outer Galaxy or radial motion of the Local Standard of Rest. We shall review the evidence for oscillations of the Galactic disk, with particular emphasis on the interplay between these oscillations and the kinematics of the solar neighbourhood.

1. Introduction

Ever since Kapteyn made the first serious attempt to construct an accurate model of the Galaxy, most investigations have started by assuming that the large-scale distribution of stars in the Galaxy is axisymmetric and stationary.

In this paper we discuss the validity of this simple assumption, *i.e.* whether there are non-axisymmetric or non-stationary distortions with characteristic scale comparable to the size of the Galactic disk. Thus we exclude small-scale irregularities due, for example, to inhomogeneous star formation, gravitational wakes induced by giant molecular clouds, tightly wrapped spiral arms, etc. We also restrict ourselves to planar distortions; in particular, we shall not discuss the warps that are known to exist in our own and other galaxies.

An arbitrary perturbation to an axisymmetric disk can be expanded in a series of terms of the form $\mathrm{Re}\{f(R,z)\exp[i(m\phi-\omega t)]\}$, where (R,ϕ,z) is the usual cylindrical coordinate system and the properties of the unperturbed disk are independent of ϕ (to ensure that the angular speed of the Galaxy is positive, $\hat{\mathbf{e}}_z$ must point towards[1] the

[1] The reader is warned that other authors use different conventions to deal with this unpleasant sign problem, including negative angular speed for the Galaxy and radial coordinates that increase towards the Galactic centre. The most satisfactory long-term solution would be to switch the north and south Galactic poles!

B. Sundelius (ed.) Dynamics of Disc Galaxies (1991) Göteborg, Sweden, pp. 71–104.

South Galactic Pole). We shall call these perturbations "oscillations". An oscillation with $m = 0$, $\omega \neq 0$ is axisymmetric but non-stationary. For $m \neq 0$ we may define the pattern speed $\Omega_p \equiv \omega/m$; to an observer in the frame rotating with the pattern speed the oscillation appears stationary. Large-scale oscillations require small azimuthal wavenumbers m. We may assume $m \geq 0$ without loss of generality.

As a preliminary exercise, consider a model of the Galaxy in which the stars and gas travel on similar elliptical streamlines with axis ratio $q \leq 1$,

$$x^2 + y^2/q^2 = \lambda^2, \tag{1}$$

with velocity

$$v_x = -\frac{v_0 y}{\lambda}, \qquad v_y = q^2 \frac{v_0 x}{\lambda}, \tag{2}$$

which yields a constant velocity along any radial direction. (This is a kinematic model only—the velocity field does not necessarily arise from any plausible dynamical model.) Suppose that the Sun lies on the major or minor axis. How can we determine the axis ratio q from observations?

The main point of this exercise is that determining q is remarkably difficult. The local velocity field and the tangent-point velocities are indistinguishable from those in axisymmetric disks. The best approach is to compare the distance distribution of a tracer population along various lines of sight, but to do this we need a good standard candle that is visible at large distances, such as Cepheids, OB stars, or carbon stars.

As an illustration of the available constraints, we consider a recent measurement of the distance d to the H_2O masers in W49(N). The source lies at longitude $\ell = 43°$ and its line-of-sight velocity is near zero with respect to the Local Standard of Rest. Hence in an axisymmetric, stationary, differentially rotating Galaxy it must lie at the same distance from the Galactic centre as the Sun. Gwinn et al. 1989 used this result to estimate the distance to the Galactic centre, $R_\odot = \frac{1}{2} d/\cos\ell$, and found a value 1.0 ± 0.2 times the best estimate for $R_\odot$ from more direct methods (Reid 1989). If instead the velocity field is non-axisymmetric (eq. 2), we expect this ratio to be $[1 + \cos^2\ell(1 - q^{\pm 2})]^{-1}$, where the upper (lower) sign applies if the Sun lies on the minor (major) axis. Therefore the corresponding limit on the axis ratio is $q > 0.73$ (0.87) (by definition $q < 1$).

The reader is encouraged to seek a better limit from other tracers, but probably elliptical disk models with an axis ratio as low as $q \simeq 0.8$ are compatible with all the data, so long as the Sun lies on the major or minor axis.

Models in which the Sun lies exactly on a symmetry axis are somewhat artificial. For a more typical position of the Sun, disk oscillations are easier to detect. There are at least three types of evidence:

(i) The average velocity of the Sun and its neighbours (the velocity of the Local Standard of Rest or LSR) may contain a component towards or away from the Galactic centre, and this motion may be detectable relative to gas and stars near the Galactic centre.

(ii) The kinematics of nearby objects relative to the LSR (as described by the velocity ellipsoid and Oort constants) may differ from the kinematics predicted for an axisymmetric, stationary disk.

(iii) The kinematics of distant objects may exhibit features not expected in an axisymmetric, stationary disk. In particular the velocity distribution relative to the LSR at longitude ℓ may not be the mirror image of the velocity distribution at $360^\circ - \ell$. The interpretation of the data is complicated, however, because all velocities are measured relative to the LSR: thus asymmetries in the velocities of distant objects can arise either from oscillations in the distant disk or from oscillations in the local disk that affect the velocity of the LSR.

The most thoughtful and comprehensive search for oscillations in the Galaxy has been carried out by Blitz and Spergel (1991a, hereafter B&S). They propose that the Galaxy is nearly axisymmetric at distances well beyond the solar radius, but that the inner Galaxy ($R \lesssim 1.5R_\odot$) participates in a large-scale $m = 2$ oscillation with pattern speed $\Omega_p = 5.5\,\mathrm{km\,s^{-1}\,kpc^{-1}}$, caused by a rotating triaxial bulge. Because of this oscillation the LSR moves outward at $14\,\mathrm{km\,s^{-1}}$ relative to the Galactic centre.

At this point we introduce some notation. The number of stars in the phase-space volume element $d\mathbf{x}d\mathbf{v}$ is $f(\mathbf{x},\mathbf{v})d\mathbf{x}d\mathbf{v}$ where f is the distribution function (abbreviated DF). We write the average of a quantity X over velocity at a given position as $\overline{X} = \int f(\mathbf{x},\mathbf{v})X d\mathbf{v} / \int f(\mathbf{x},\mathbf{v})d\mathbf{v}$. The velocity-dispersion tensor is $\sigma_{ij} \equiv \overline{(v_i - \overline{v_i})(v_j - \overline{v_j})}$. The velocity ellipsoid is the three-dimensional surface on which the quadratic $x_i\sigma_{ij}^{-1}x_j$ is unity; the orientation and shape of the velocity ellipsoid provide a measure of the residual velocity distribution.

2. The stationary axisymmetric disk

We begin with a review of the local kinematics of a stationary, axisymmetric galaxy, in which both the potential $\Phi(R,z)$ and the DF are assumed to be independent of azimuth and time. By Jeans' theorem the DF depends only on the isolating integrals of motion. Any DF that depends only on the two analytic integrals $E = \frac{1}{2}(v_R^2 + v_\phi^2 + v_z^2) + \Phi(R,z)$ and $L_z = Rv_\phi$ is symmetric in v_R and in v_z at a given spatial location, in other words the three axes of the velocity ellipsoid are aligned with the (R,ϕ,z) coordinate axes ($\sigma_{R\phi} = \sigma_{Rz} = \sigma_{\phi z} = 0$). Moreover $\overline{v_R} = \overline{v_z} = 0$. However, most orbits in most axisymmetric galaxy-like systems have a third integral I so in general the DF is a function of E, L_z and I. Usually the integral I is invariant under the change $(v_R, v_z) \to (-v_R, -v_z)$—even though an explicit expression for I is not usually available, an orbit with given integrals E, L_z, I spends an equal fraction of its time in the neighbourhoods of the phase-space points $(R,\phi,z,v_R,v_\phi,v_z)$ and $(R,\phi,z,-v_R,v_\phi,-v_z)$. This symmetry implies that the velocity ellipsoid is aligned with the rotation direction ($\sigma_{R\phi} = \sigma_{\phi z} = 0$) and the mean velocity is in the azimuthal direction ($\overline{v_R} = \overline{v_z} = 0$). The argument is not rigorous because integrals I can exist that do not have this symmetry, if resonances are present.

Thus if both the potential and the DF are stationary and axisymmetric, it is reasonable to expect that $\sigma_{R\phi} = \sigma_{\phi z} = 0$. Then two of the principal axes of the velocity ellipsoid lie in the (R,z) plane and the third lies in the direction of rotation.

If the DF is symmetric about the plane $z = 0$, then there are symmetries in this plane whatever the nature of the third integral may be: (i) $\sigma_{\phi z} = \sigma_{Rz} = 0$; (ii) the DF

is symmetric in v_z. If I is invariant under $(v_R, v_z) \to (-v_R, -v_z)$ then the DF is also symmetric in v_R.

In contrast, the distribution in $v_\phi - \overline{v_\phi}$ is not required to be symmetric. Generally, the stars with $v_\phi < \overline{v_\phi}$ come from inside the solar circle, where the density and velocity dispersion are greater than outside. The density and dispersion gradients produce an asymmetry of the v_ϕ-distribution about its mean, as well as the classical asymmetric drift (*i.e.* $\overline{v_\phi} - v_c \propto \sigma_{RR}$ where $v_c(R)$ is the circular speed at radius R).

The distribution in $v_\phi - \overline{v_\phi}$ becomes simpler in the limit $\sigma_{\phi\phi} \ll v_c^2$. In this case the distribution is approximately symmetric and moreover (e.g. Binney and Tremaine 1987)

$$\frac{\sigma_{\phi\phi}}{\sigma_{RR}} = -\frac{B}{(A-B)}, \tag{3}$$

where

$$A = \tfrac{1}{2}(v_c/R - dv_c/dR)_{R_\odot}, \quad B = -\tfrac{1}{2}(v_c/R + dv_c/dR)_{R_\odot}, \tag{4}$$

are the usual Oort constants. For a flat rotation curve ($v_c(R)$ independent of R), which is an accurate representaton of the rotation curve of the Galaxy in the region of interest (e.g. Fich and Tremaine 1991), this relation implies $\sigma_{\phi\phi}/\sigma_{RR} = \frac{1}{2}$. Since deviations from the relation (3) might provide evidence of oscillations, it is important to understand how accurately it is expected to be satisfied in the solar neighbourhood.

To provide a simple example, we average over z and v_z and so consider a DF $f(E_t, L_z)$ where $E_t = \frac{1}{2}v_R^2 + v_\phi^2 + \Phi(R)$ is the energy in motion parallel to the disk plane. A sufficiently general form for the DF is

$$f(E_t, L_z) = g(L_z)\exp\{-\beta(L_z)[E_t - E_c(L_z)]\}, \tag{5}$$

where E_c is the energy of a circular orbit of angular momentum L_z. "Typical" galaxy disks have a surface brightness profile $\mu \propto \exp(-R/h)$ where h is the scale length (Freeman 1970), a circular speed independent of radius, and a radial velocity dispersion $\sigma_{RR} \propto \mu$ (if the mass-to-light ratio and z-averaged σ_{RR}/σ_{zz} are independent of radius; this proportionality implies that the thickness of the disk is independent of radius, consistent with observations of van der Kruit and Searle 1982). To get a constant circular speed we take $\Phi(R) = v_c^2 \ln R$. We also take $g(L_z)$ =constant and $\beta(L_z) \propto \exp[L_z/(hv_c)]$ (these choices ensure that $\mu \propto \sigma_{RR} \propto \exp(-R/h)$ when the velocity dispersion is small). A very similar DF is described by Newton (1986) and Binney (1987). We may now evaluate the velocity moments of f at radius R in powers of $b = [v_c^2\beta(Rv_c)]^{-1}$:

$$\begin{aligned}
\frac{\overline{v_\phi}}{v_c} &= 1 + b(\tfrac{1}{4} - \xi) + b^2(-\tfrac{19}{8}\xi^3 + \tfrac{33}{16}\xi^2 + \tfrac{17}{48}\xi + \tfrac{1}{32}) + \mathrm{O}(b^3), \\
\frac{\sigma_{\phi\phi}}{v_c^2} &= \tfrac{1}{2}b + b^2(\tfrac{15}{8}\xi^2 - \tfrac{9}{8}\xi - \tfrac{1}{8}) + \mathrm{O}(b^3), \\
\frac{\sigma_{RR}}{v_c^2} &= b + b^2(\tfrac{5}{4}\xi^2 - \tfrac{1}{4}\xi) + \mathrm{O}(b^3), \\
\frac{\sigma_{\phi\phi}}{\sigma_{RR}} &= \tfrac{1}{2} + b(\tfrac{5}{4}\xi^2 - \xi - \tfrac{1}{8}) + \mathrm{O}(b^2),
\end{aligned} \tag{6}$$

where $\xi = R/h$.

We recover the usual formula (3) for the axis ratio of the dispersion tensor to leading order in b, but the next-order term has a large coefficient. Thus, taking conservative values $\xi = 2$, $b = 0.03$ (corresponding to $\sigma_{RR}^{1/2} = 41\,\mathrm{km\,s^{-1}}$ for $v_c = 220\,\mathrm{km\,s^{-1}}$), we have $\sigma_{\phi\phi}/\sigma_{RR} = 0.59$, which differs by 17% from the classical value $\frac{1}{2}$. Increasing ξ or b rapidly increases this discrepancy; for example, $\xi = 2.5$ implies $\sigma_{\phi\phi}/\sigma_{RR} = 0.66$. Note that the axis ratio is always increased by the $O(b)$ correction term (so long as $\xi > 0.91$, which is certainly true in the solar neighbourhood).

Since the rotation curve of the Galaxy is nearly flat in the solar neighbourhood, these results imply that the axis ratio is likely to exceed $\frac{1}{2}$. However, observations suggest that the axis ratio is less than $\frac{1}{2}$, although the evidence is not clear-cut. The sources quoted by Kerr and Lynden-Bell (1986) give values for $\sigma_{\phi\phi}/\sigma_{RR}$ ranging from 0.36 to 0.50 with a mean of 0.42. A recent investigation by Ratnatunga and Upgren (1991) of the Vyssotski K and M dwarfs yields $\sigma_{\phi\phi}/\sigma_{RR}$ for the two (Gaussian) components of 0.37 (young disk) and 0.44 (old disk); the entire sample has 0.45. An analysis of stars from the Gliese (1969) catalog (absolute magnitudes and line-of-sight velocities of quality "C" or better, white dwarfs excluded, only one component of multiple systems kept) gives $\sigma_{\phi\phi}/\sigma_{RR} = 0.62$ ($\sigma_{RR}^{1/2} = 42\,\mathrm{km\,s^{-1}}$) for 602 stars. (Another catalogue of 1004 stars, in which poorer-quality M_V values were also allowed, was also analyzed. No significant differences between the two data sets were ever found in this or any of the other measurements we describe in this paper.)

The resolution of this discrepancy between theory and observation (pointed out by Binney 1987) is unclear. It is possible that many determinations do not account fully for the tail towards negative v_ϕ that we expect to be present in the data (for example, velocities are sometimes fit to a Gaussian distribution). Another possibility, as we discuss below, is that the axis ratio may be affected by oscillations.

An alternative, model-independent way to analyze the axis ratio problem employs the velocity moments of the collisionless Boltzmann equation. Assuming a stationary, axisymmetric galaxy, we eliminate the potential from the v_R- and $v_R v_\phi$-moments of this equation (Binney and Trèmaine 1987, eqs. 4-29a and 4-47). In the symmetry plane, where $\sigma_{Rz} = 0$, we find

$$\begin{aligned}\frac{\sigma_{\phi\phi}}{\sigma_{RR}} &= \frac{\overline{v_\phi} + R\overline{v_\phi}_{,R}}{2\overline{v_\phi}} + \frac{1}{2\sigma_{RR}\overline{v_\phi}}\left[\frac{1}{\nu R}\frac{\partial(\nu R^2\sigma_{RR\phi})}{\partial R} + \frac{R}{\nu}\frac{\partial(\nu\sigma_{R\phi z})}{\partial z} - \sigma_{\phi\phi\phi}\right] \\ &= \frac{-\overline{B}}{\overline{A}-\overline{B}} + O\left(\frac{\sigma_{ijk}}{\sigma_{RR}v_c}\right),\end{aligned} \tag{7}$$

where $_{,R}$ denotes $\partial/\partial R$ and ν is the density. Equation (7) shows that the corrections to equation (3) may be thought of as arising from two sources: (i) the third moments $\sigma_{RR\phi}$, $\sigma_{R\phi z}$, and $\sigma_{\phi\phi\phi}$, which would vanish if the distribution in v_ϕ were symmetric; (ii) the distinction between the Oort constants A and B defined in equations (4), and the "observed" constants $\overline{A}$ and $\overline{B}$, which are obtained by replacing the circular speed v_c by the mean speed $\overline{v_\phi}$ in equations (4). Notice that the right side of equation (7) is

difficult to evaluate from local observations, because it depends on spatial gradients of the third moments, which are large and uncertain.

The difference $v_c - \overline{v_\phi}$ between the circular speed and the mean speed is known as the asymmetric drift (see, e.g. Jahreiss and Wielen 1983). For our model DF (5), we can obtain the asymmetric drift from equations (6):

$$\overline{v_\phi} = v_c + \frac{\sigma_{RR}}{v_c}(\tfrac{1}{4} - \xi) + \frac{\sigma_{RR}^2}{v_c^3}(-\tfrac{9}{8}\xi^3 + \tfrac{3}{2}\xi^2 + \tfrac{5}{12}\xi + \tfrac{1}{32}) + \mathrm{O}(\sigma_{RR}^3/v_c^5). \tag{8}$$

(Recall that σ_{RR} is the *squared* velocity dispersion.) The term linear in σ_{RR} is the one usually used to estimate v_c from $\overline{v_\phi}$ (a full three-dimensional calculation shows that a correction term should also be included if $\partial(\overline{v_R v_z})/\partial z$ is non-zero; see, e.g., Binney and Tremaine 1987). The error in $\overline{v_\phi}$ arising from the quadratic term can be as large as $-1.7\,\mathrm{km\,s^{-1}}$ for $\sigma_{RR}^{1/2} = 40\,\mathrm{km\,s^{-1}}$ (with $\xi = 2.5$, about the largest plausible value); while this correction is not negligible it is probably not a major source of uncertainty in $\overline{v_\phi}$. [2]

Equations (6) can also be used to estimate the corrections for dispersion that are needed when measuring the Oort constants from the differential motions of old disk stars. Such data measure not v_c and its local gradient, but rather $\overline{v_\phi}$: hence a dispersion-dependent correction is required to obtain the true Oort constants for the circular speed curve $v_c(R)$. In our model, which is based on a flat circular speed curve ($A = -B = \frac{1}{2}v_c/R_\odot$), the observed values $\overline{A}$ and $\overline{B}$ are given by

$$\overline{A} = A[1 + b(\tfrac{1}{4} + \tfrac{1}{4}\xi - \xi^2) + \mathrm{O}(b^2)], \quad \overline{B} = B[1 + b(\tfrac{1}{4} - \tfrac{9}{4}\xi + \xi^2) + \mathrm{O}(b^2)]. \tag{9}$$

For typical values $\xi = 2$ and $b = 0.03$ we have $\overline{A} = 0.90A$, $\overline{B} = 0.99B$. So A can be underestimated by 10% or more, whereas B is affected only a little (see also Lewis 1990).

3. The effect of oscillations on local kinematics

3. 1. OORT CONSTANTS

We first generalize the Oort constants for a non-axisymmetric or non-stationary disk (Milne 1935, Chandrasekhar 1942). The mean velocity of the stars at a position in the Galactic plane $\mathbf{r} = (x_1, x_2)$ relative to the Sun can be expanded in a Taylor series,

$$\overline{v}_i \equiv H_{ij}x_j + \mathrm{O}(x^2), \tag{10}$$

where the coordinate axes $\hat{\mathbf{e}}_1$, $\hat{\mathbf{e}}_2$ point towards $\ell = 0°$ and $\ell = 90°$. Without loss of generality we may write

$$\mathbf{H} = \begin{pmatrix} K + C & A - B \\ A + B & K - C \end{pmatrix}; \tag{11}$$

[2] By constructing a suitable combination of σ_{RR} and $\sigma_{\phi\phi}$, it is possible to eliminate the $\mathrm{O}(\sigma_{RR}^2)$ term, facilitating a linear extrapolation to determine v_c from $\overline{v_\phi}$. For example, at $\xi = 2$, $\overline{v_\phi} = v_c - (1.38\sigma_{RR} + 0.74\sigma_{\phi\phi})/v_c + \mathrm{O}(\sigma_{RR}^3/v_c^5)$. Such a relation might be an improvement over the usual formula (8); at the least use of such alternate formulae would provide a measure of the error from nonlinear terms.

we have simply written the four components of the matrix **H** in terms of the four (possibly time-dependent) parameters A, B, C, K. Note that K measures the divergence, $\nabla \cdot \bar{\mathbf{v}} = 2K$, while B measures the vorticity, $\hat{\mathbf{e}}_3 \cdot \nabla \times \bar{\mathbf{v}} = 2B$, and the shear tensor $\overline{v_i}_{,k} + \overline{v_k}_{,i} - \delta_{ik}\overline{v_j}_{,j}$ depends only on A and C (here $\overline{v_i}_{,k} \equiv \partial \overline{v_i}/\partial x_k$ and we sum over repeated indices). The mean line-of-sight velocity $\overline{v}_{\rm rad}$ and proper motion $\overline{\mu}$ of objects at $(x_1, x_2) = r(\cos\ell, \sin\ell)$ are then given by (e.g. Chandrasekhar 1942):

$$\begin{aligned} \overline{v}_{\rm rad}/r &= K + A\sin 2\ell + C\cos 2\ell \equiv K + \sqrt{A^2+C^2}\sin 2(\ell - \psi_v), \\ \overline{\mu} &= B + A\cos 2\ell - C\sin 2\ell \equiv B + \sqrt{A^2+C^2}\cos 2(\ell - \psi_v), \end{aligned} \tag{12}$$

with $\tan 2\psi_v = -C/A$. The angle ψ_v is the longitude of the kinematic Galactic centre. In polar coordinates

$$\begin{aligned} 2A &= \overline{v_\phi}/R - \overline{v_R}_{,\phi}/R - \overline{v_\phi}_{,R}, \\ 2B &= -\overline{v_\phi}/R + \overline{v_R}_{,\phi}/R - \overline{v_\phi}_{,R}, \\ 2C &= -\overline{v_R}/R - \overline{v_\phi}_{,\phi}/R + \overline{v_R}_{,R}, \\ 2K &= \overline{v_R}/R + \overline{v_\phi}_{,\phi}/R + \overline{v_R}_{,R}. \end{aligned} \tag{13}$$

If the disk is stationary and axisymmetric, then $K = C = 0$, and the equations reduce to the usual formulae (4) for the Oort constants A and B.

A disk in which $K = \psi_v = 0$ throughout is not necessarily stationary and axisymmetric (a counterexample is the velocity field of eq. 2). Any disk in which $\nabla \cdot \bar{\mathbf{v}} = 0$ and $\overline{v_R}_{,R} = 0$ has $K = \psi_v = 0$.

Two unfortunate problems arise when we attempt to assess the observational constraints on K and ψ_v (or C): (i) Some authors fit to models with variable K but zero C, while others fit to zero K but variable C. There is no theoretical reason to prefer one over the other, so models should always fit to both. (ii) Some authors fit for a constant expansion term, $\overline{v}_{\rm rad} = k$ rather than rK. The k-term accounts for a constant offset in velocity; such an offset is a useful component of the fit but does not substitute for the K-term.

Observations indicate that K and ψ_v are small near the Sun once the local system (Gould's Belt) is excluded. Typically this requires removing all stars within 0.3–0.6 kpc from the Sun. From 240 OB stars at distances of 0.45–2 kpc from the Sun, Tsioumis and Fricke (1979) found $\psi_v = 1.5 \pm 3°$* and $K = 2.1 \pm 1.7\,\mathrm{km\,s^{-1}\,kpc^{-1}}$* (we use asterisks to denote values that will enter into the weighted means derived below). du Mont (1977) reports $\psi_v = 10 \pm 7°$* for 124 FK4 stars between 0.3 and 1.3 kpc distant; since du Mont uses only proper motions he is insensitive to K. Using line-of-sight velocities of open clusters (r = 0.3–2 kpc), Lynga and Palouš (1987) found $K = 2.9 \pm 2.5\,\mathrm{km\,s^{-1}\,kpc^{-1}}$*, $\psi_v = 2.5 \pm 6.6°$* for clusters older than 30 Myr, whereas younger clusters give $K = -2.6 \pm 1.0\,\mathrm{km\,s^{-1}\,kpc^{-1}}$ and $\psi_v = -9.7 \pm 2.9°$ (we do not use the younger sample in our weighted means since it is less well-mixed and more susceptible to local oscillations). A similar investigation of 105 open clusters by Hron (1987) reveals "no significant" K-term either; we shall quantify this result as $K = 0 \pm 1.5\,\mathrm{km\,s^{-1}\,kpc^{-1}}$* (the error

is the quoted error in his measurement of Oort's A). From Cepheids with $r < 5\,\mathrm{kpc}$ Kraft and Schmidt (1963) found $K = -1.5 \pm 0.6\,\mathrm{km\,s^{-1}\,kpc^{-1}}$*, although they prefer to interpret their results in terms of a constant radial-velocity error k (possibly arising from expansion of the stellar envelope). Humphreys' (1970) sample of 333 supergiants with $r > 0.5\,\mathrm{kpc}$ yields $k = -0.4 \pm 0.5\,\mathrm{km\,s^{-1}}$, or $K = -0.2 \pm 0.3\,\mathrm{km\,s^{-1}\,kpc^{-1}}$*. None of the last three authors incorporated a C-term in their models. The classical analysis of Cepheids by Joy (1939) (this time analyzed with a C-term but no K-term!) yields $\psi_v = -2.4 \pm 1.3°$*. The starred estimates are plotted in Figure 1.

We do not feel able to offer realistic assessments of the errors in these measurements of K and ψ_v. We have adopted the following arbitrary procedure: we assume that each measurement is subject to random errors described by the quoted error limits. In addition, we assume that there is a random error of unknown variance (the "external" error) that affects each measurement and that is not included in the quoted errors; this variance is chosen to fit the dispersion between the results of different authors (cf. Godwin and Lynden-Bell 1987 for a similar approach). Combining the two errors to estimate the total error, we find the weighted mean and its standard deviation, then arbitrarily *double* the standard deviation to obtain an error estimate that we call the "likely error". The doubling is simply a crude effort to obtain more realistic bounds on the weighted mean.

Using this procedure on the starred estimates above, we find the weighted means and likely errors:

$$K = -0.35 \pm 0.5\,\mathrm{km\,s^{-1}\,kpc^{-1}}, \qquad \psi_v = -1.3 \pm 2.3°. \tag{14}$$

These limits are plotted in Figure 1. The range in Oort's constant C implied by the limits (14) is $0.6 \pm 1.1\,\mathrm{km\,s^{-1}\,kpc^{-1}}$. The B&S model predicts $K = 0.4\,\mathrm{km\,s^{-1}\,kpc^{-1}}$ and $\psi_v = -3.8°$, agreeing within 1.7 and 1.1 "likely errors" with the observations. The radial gradient in radial velocity, $\overline{v_{R,R}} = K + C$ is then less than $2\,\mathrm{km\,s^{-1}\,kpc^{-1}}$ in absolute value. Thus, differential motions in the solar neighbourhood provide no indication of deviations from stationary circular motion outside the local system (r <300–600 pc).

3. 2. THE RADIAL VELOCITY OF THE LSR

The Local Standard of Rest or LSR is the frame travelling with the mean velocity of the stars in the solar neighbourhood (because of the asymmetric drift the mean velocity depends on the dispersion of the stellar population; thus in a stricter sense the LSR travels at the mean velocity of a hypothetical population with negligible dispersion). A non-zero radial velocity of the LSR with respect to the Galactic centre would be evidence for oscillations.

We first estimate the radial velocity of the LSR relative to the Sun, $v_{R,\mathrm{LSR}} - v_{R\odot}$. The classic observational summary is given by Delhaye (1965), who gives two estimates, $v_{R,\mathrm{LSR}} - v_{R\odot} = 10.4\,\mathrm{km\,s^{-1}}$ (standard solar motion) and $9\,\mathrm{km\,s^{-1}}$ (basic solar motion), *i.e.* the Sun moves inwards relative to the LSR. Delhaye finds no detectable dependence of the radial velocity of the LSR on the velocity dispersion, which implies that small-scale

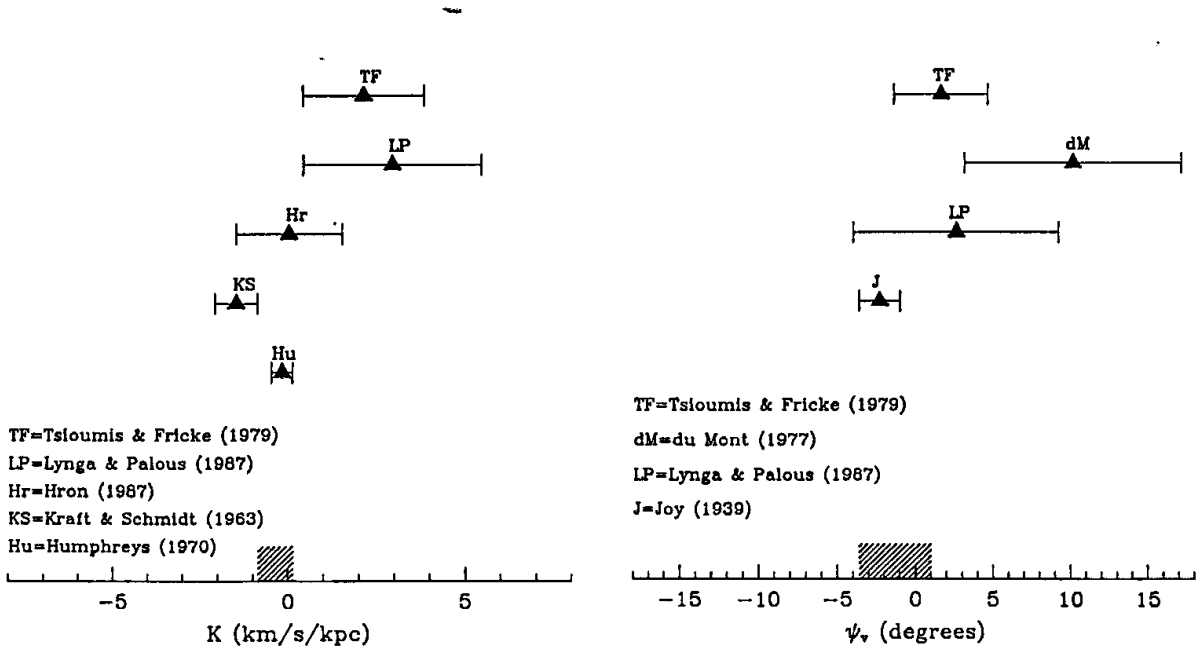

Figure 1. Determinations of (left) Oort's constant K and (right) the longitude of the kinematic Galactic centre ψ_v (eqs. 10–12). The estimates shown are the ones marked by asterisks in the text; error estimates are those of the authors cited. The midpoint of the shaded region on the horizontal scale denotes the best value and the range of the shaded region denotes the likely error. See text for details.

oscillations (due, for example, to local spiral structure, whose effects would be washed out in a high-dispersion population) do not contribute to the mean radial velocity.

A more recent analysis by Ratnatunga and Upgren (1991) of the Vyssotsky K and M dwarfs finds $v_{R,\mathrm{LSR}} - v_{R\odot} = 8.1 \pm 1.4\,\mathrm{km\,s^{-1}}$*. This agrees well with Jahreiss and Wielen's (1983) estimate of $8 \pm 3\,\mathrm{km\,s^{-1}}$ (our error estimate), from older, less extensive data for these stars. Murray et al. (1986) measured proper motions for $\sim$ 6000 stars towards the South Galactic Pole: using their parallaxes and proper motions for stars with B−V redder than 0.8, we obtain a solar motion of $10.4 \pm 2\,\mathrm{km\,s^{-1}}$* (the error bar includes the estimated uncertainty in the zero point of the proper motion system). Hron (1987) finds $7.4 \pm 2\,\mathrm{km\,s^{-1}}$* for the best quality open clusters in his sample; he also provides a list of many previous determinations of the solar motion. Jaschek and Valbousquet (1991) determine the solar motion using 5800 stars from the "Bright Star Catalog". They find $v_{R,\mathrm{LSR}} - v_{R\odot} = 11.3 \pm 0.8\,\mathrm{km\,s^{-1}}$* (straight mean over spectral types), with no significant dependence on spectral type, age or distance.

As an independent check, we have analyzed the Gliese (1969) catalogue of nearby stars. We find $v_{R,\mathrm{LSR}} - v_{R\odot} = 11.4 \pm 1.0\,\mathrm{km\,s^{-1}}$*. Dividing the sample into roughly equal thirds by ranking in $|v_z|$ gives 11.3 ± 1.3, 9.1 ± 1.5 and $13.8 \pm 4.1\,\mathrm{km\,s^{-1}}$ for stars with vertical speeds below 6, between 6 and 15, and above $15\,\mathrm{km\,s^{-1}}$ respectively. Thus

we confirm that there is no significant dependence of the radial motion of the LSR on velocity dispersion.

Combining the starred measurements as described in the previous section, we obtain a weighted mean and likely error of $v_{R,\mathrm{LSR}} - v_{R\odot} = 10.3 \pm 1.3\,\mathrm{km\,s^{-1}}$ (the likely error estimate includes a contribution from the estimated external error of $0.8\,\mathrm{km\,s^{-1}}$). The standard solar motion of $10.4\,\mathrm{km\,s^{-1}}$ lies well within the likely error, and is the value we shall use in the rest of this paper. (Incorporating all the determinations listed by Hron gives $8.7 \pm 1.1\,\mathrm{km\,s^{-1}}$, with an external error of of $1.4\,\mathrm{km\,s^{-1}}$.) Figure 2 shows all of the starred estimates, as well as the standard solar motion and the range implied by our best estimate and likely error.

The velocity of the Sun relative to the local interstellar medium can be measured by studying HII regions near the Galactic centre and anticentre directions. Fich et al. (1989) found that the HII regions in their sample (mostly in the anticentre direction, with a mean distance of 2.6 kpc) had a mean inward velocity of $4.2 \pm 1.5\,\mathrm{km\,s^{-1}}$ relative to the LSR. This motion might be regarded as evidence for an oscillation with a non-zero radial velocity gradient, $\overline{v_R}_{,R} \simeq -4.2\,\mathrm{km\,s^{-1}}/2.6\,\mathrm{kpc} = -1.6\,\mathrm{km\,s^{-1}\,kpc^{-1}}$, or it might arise from a small-scale oscillation to which the gas is responding more strongly than the stars.

The motion of the interstellar medium inside the solar circle can be studied from 21 cm absorption in the Galactic centre radio source (e.g. Radhakrishnan and Sarma 1980). There is a strong absorption feature arising from gas all along the line of sight to the Galactic centre, with mean velocity relative to the LSR of $-0.23 \pm 0.06\,\mathrm{km\,s^{-1}}$ and dispersion $5\,\mathrm{km\,s^{-1}}$. Assuming that the gas is approximately uniformly distributed in radius, the narrowness of the feature implies that the radial velocity $\overline{v_R}$ varies by $\lesssim 5\,\mathrm{km\,s^{-1}}$ over the distance to the Galactic centre of about 8 kpc, corresponding to an average gradient $|\overline{v_R}_{,R}| \lesssim 5\,\mathrm{km\,s^{-1}}/8\,\mathrm{kpc} = 0.6\,\mathrm{km\,s^{-1}\,kpc^{-1}}$, which is much smaller than the limit derived from Oort's constants in the previous section, but also less local.

We now discuss the determination of the radial velocity of the LSR $v_{R,\mathrm{LSR}}$. The simplest determination is from globular clusters, which we can see throughout the Galaxy, and which we can reasonably assume to form a stationary system. Given a catalogue of heliocentric line-of-sight velocities v_{rad}, we can derive the Sun's outwards motion as $v_{R\odot} = \langle v_{\mathrm{rad}} \cos\ell \cos b\rangle / \langle \cos^2\ell \cos^2 b\rangle$, where $\langle\cdot\rangle$ denotes an average over the clusters. From Thomas's (1989) compilation of the available data, we obtain $v_{R\odot} = -7.9 \pm 17\,\mathrm{km\,s^{-1}}$ with respect to the 27 clusters within 10° of the Galactic centre which have measured radial velocities. Using all 115 clusters with line-of-sight velocities yields $v_{R\odot} = -13 \pm 13\,\mathrm{km\,s^{-1}}$. Correcting for the standard solar motion we find $v_{R,\mathrm{LSR}} = 2 \pm 13\,\mathrm{km\,s^{-1}}$ and $-3 \pm 13\,\mathrm{km\,s^{-1}}$*. Thus, the globular cluster kinematics provide no evidence for radial LSR motion, although the limits are not very tight.

One can also attempt to measure the radial velocity of the LSR by comparing the velocity of the LSR to the mean velocity of high-velocity stars (with $\sigma_{RR}^{1/2}$ in excess of $100\,\mathrm{km\,s^{-1}}$), which presumably participate less strongly in any radial oscillation. Unfortunately, the high dispersion implies that a large sample of stars is needed, and the statistical error in existing samples is too large for a useful estimate: using the radial

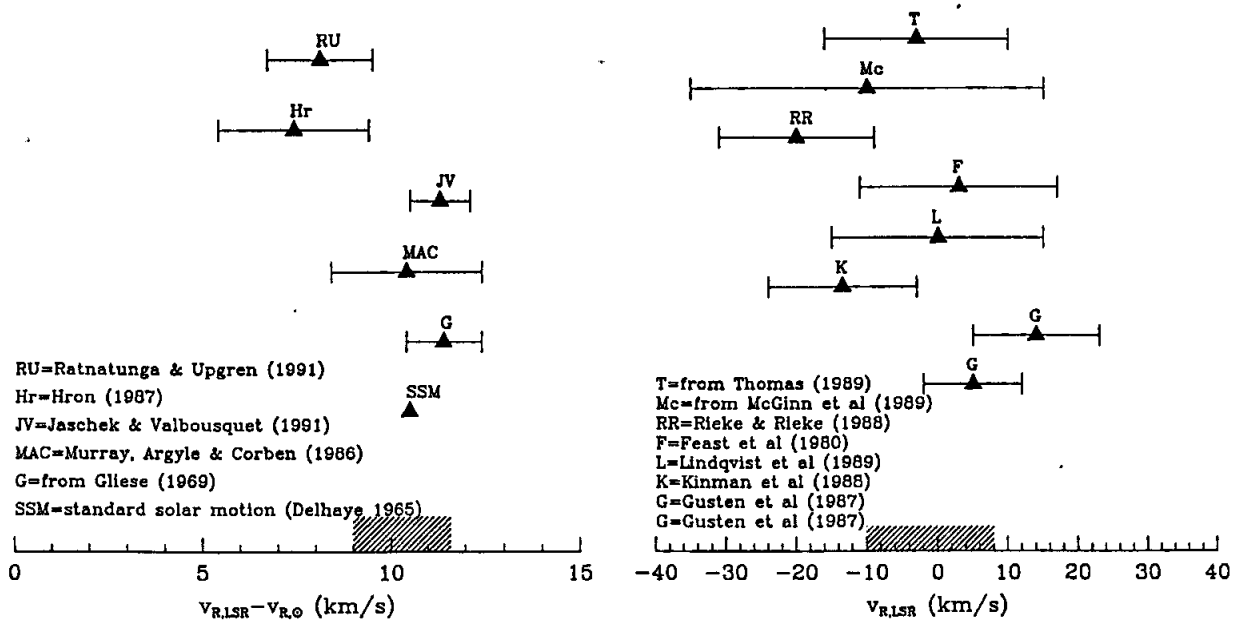

Figure 2. Determinations of (left) the radial component of the velocity of the LSR relative to the Sun and (right) the radial velocity of the LSR. The estimates shown are those marked by asterisks in the text; error estimates are those of the authors cited. The standard solar motion (Delhaye 1965) is also marked. The shaded regions denote the range allowed by our best estimate and likely error. See text for details.

velocities for high proper motion stars listed by Fouts and Sandage (1986), we find the mean velocity relative to the Sun of 311 stars with ultraviolet excess $\delta(0.6) > 0.15$ to be $\overline{v_R} - v_{R\odot} = 7 \pm 13\,\mathrm{km\,s^{-1}}$; the 330 stars in the Carney and Latham (1987) sample with [Fe/H] < -1 give $14 \pm 12\,\mathrm{km\,s^{-1}}$. Both numbers are consistent with the standard solar motion determined from low-dispersion populations, but the errors are large enough that a relative drift between the high- and low-dispersion populations as large as 10–15 $\mathrm{km\,s^{-1}}$ cannot be excluded.

Ideally, to determine the radial velocity of the LSR we would like to measure the mean radial velocity of a well-mixed and complete population of tracers localized near the Galactic centre. Unfortunately, a number of complications are present:

(i) The stellar populations near the Galactic centre are kinematically hot, with line-of-sight velocity dispersions $\sim 100\,\mathrm{km\,s^{-1}}$, so that many objects are required in order to measure the mean velocity accurately (~ 1000 to measure $v_{R,\mathrm{LSR}}$ within $3\,\mathrm{km\,s^{-1}}$).

(ii) The rotation speeds of cold populations remain high even at small distances from the centre. Therefore any slight asymmetry in the longitude distribution of the sample will bias its mean line-of-sight velocity.

(iii) Gas motions are very complicated near the centre. Maps of atomic or molecular gas reveal many clumps, asymmetries, and "forbidden" (in an axisymmetric system)

motions. (But see Binney et al. 1991 for a coherent dynamical model.)

(iv) Optical measurements of objects near the Galactic centre can only be made in a few windows where the extinction is relatively low. Recent work on the 2.3μ $2-0$ vibration band head of the CO molecule has provided the first measurements of stellar velocities in the central regions of the Galaxy.

(v) There is no strong theoretical reason to expect that the Galactic centre—as measured by the peak of the near-infrared emission—is necessarily the appropriate reference point. For example, there might be an oscillation localized to the central few hundred parsecs while the bulk of the Galaxy outside that radius was stationary and axisymmetric.

Line-of-sight velocities have been measured over the past few years for stars within a few parsecs of the Galactic centre. McGinn et al. (1989) have measured the mean velocity and velocity dispersion in the central 10 pc using integrated light spectra around the 2.3μ CO band head, which is mostly from low-mass stars. They find $v_{R,\mathrm{LSR}} = -10 \pm 25\,\mathrm{km\,s^{-1}}$* if the centre coincides with the source IRS 16; however, the result is sensitive to the chosen centre because the stars rotate and the uncertainty of $\pm 10''$ in the position of the centre implies an additional uncertainty of $\pm 10\,\mathrm{km\,s^{-1}}$ in $v_{R,\mathrm{LSR}}$. Additional evidence of uncertainty is that measurements at four minor axis positions yield $v_{R,\mathrm{LSR}} = -47 \pm 8\,\mathrm{km\,s^{-1}}$. Rieke and Rieke (1988) measured 54 stars in the central 6 parsecs and obtained $v_{R,\mathrm{LSR}} = -20 \pm 11\,\mathrm{km\,s^{-1}}$* (as quoted in McGinn et al. 1989). At larger radii (150 pc), OH/IR stars appear to be at rest relative to the LSR (Lindqvist et al. 1989) within $\sim 15\,\mathrm{km\,s^{-1}}$; we assign these $v_{R,\mathrm{LSR}} = 0 \pm 15\,\mathrm{km\,s^{-1}}$*. A sample of planetary nebulae, Mira stars, and OH/IR stars within $|\ell| \leq 2°$ of the Galactic centre yields $v_{R,\mathrm{LSR}} = 3 \pm 14\,\mathrm{km\,s^{-1}}$* (Feast et al. 1980), and 109 planetary nebulae within 5° of the centre yield $v_{R,\mathrm{LSR}} = -13.6 \pm 10.5\,\mathrm{km\,s^{-1}}$* (Kinman et al. 1988). The sample volume for this last result is large enough that there is concern that the mean velocity might be biased by any large-scale oscillation.

The kinematics of the gas near the galactic centre is very complicated. B&S offer several arguments based on the Galactic centre molecular gas that suggest a positive velocity for the LSR. (i) The average velocities of CO and ^{13}CO emission within $100'$ of the centre are $19\,\mathrm{km\,s^{-1}}$ and $11\,\mathrm{km\,s^{-1}}$ respectively. However, most of the gas is at positive longitudes, where velocities from Galactic rotation are positive (see Figure 21 of Oort 1977), so the velocities may reflect the central rotation curve rather than motion of the LSR. (ii) A number of features in the molecular gas can be modelled by an "expanding molecular ring" with a radius of about 200 pc (Oort 1977, Liszt and Burton 1978, 1980). The features associated with the ring at $\ell = 0$ lie at velocities of $165\,\mathrm{km\,s^{-1}}$ and $-135\,\mathrm{km\,s^{-1}}$ with respect to the LSR. B&S point out that the two features would be symmetric relative to the centre, as one would expect for a circular or elliptical expanding ring, if the LSR were receding from the Galactic centre at $v_{R,\mathrm{LSR}} = 15\,\mathrm{km\,s^{-1}}$. Like Oort (1977), we do not find the asymmetry surprising given the irregular motion of the gas near the Galactic centre and therefore we do not feel that it provides strong evidence for outward motion of the LSR. (iii) The Galactic centre is surrounded by a lumpy ring of neutral gas with a radius of about 2 pc (Güsten et al. 1987). The

velocity field of the ring suggests rotation, and Güsten et al. derive maximum rotational velocities of $137 \pm 8\,\mathrm{km\,s^{-1}}$ and $-110 \pm 5\,\mathrm{km\,s^{-1}}$ relative to the LSR defined by the standard solar motion; B&S point out that the asymmetry suggests that the LSR is moving outward relative to the Galactic centre at about $v_{R,\mathrm{LSR}} = 13 \pm 9\,\mathrm{km\,s^{-1}}$*. However, the asymmetry arises because Güsten et al. introduced a warped ring model to account for the different shape of the approaching and receding rotation curves. The peaks in the observed velocities, before correcting for the presumed warp, are at $100 \pm 5\,\mathrm{km\,s^{-1}}$ and $-90 \pm 5\,\mathrm{km\,s^{-1}}$ relative to the standard LSR, consistent with $v_{R,\mathrm{LSR}} = 5 \pm 7\,\mathrm{km\,s^{-1}}$*. Our belief is that the velocity field in the ring is not regular enough to distinguish these possibilities, so we have included both in determining our mean estimate.

Combining the estimates marked by an asterisk according to the prescription in §3.1, we arrive at a weighted mean and likely error

$$v_{R,\mathrm{LSR}} = -1 \pm 9\,\mathrm{km\,s^{-1}}, \tag{15}$$

including an estimated external error of $5\,\mathrm{km\,s^{-1}}$. All of the starred estimates, as well as the range implied by the best estimate and likely error, are shown in Figure 2. For comparison, B&S estimate $v_{R,\mathrm{LSR}} = 14\,\mathrm{km\,s^{-1}}$, which differs from our result by 1.7 times the likely error.

Some other constraints on $v_{R,\mathrm{LSR}}$ are discussed in §4.

3. 3. VERTEX DEVIATION

We have argued in §2 that $\sigma_{R\phi} = 0$ in a stationary, axisymmetric galaxy. When oscillations are present, this component of the velocity-dispersion tensor may be non-zero; the vertex deviation ℓ_v is the Galactic longitude of the largest principal axis of the velocity ellipsoid and is given by

$$\tan(2\ell_v) = -2\frac{\sigma_{R\phi}}{\sigma_{RR} - \sigma_{\phi\phi}}. \tag{16}$$

We now derive a theoretical estimate of the vertex deviation. We multiply the collisionless Boltzmann equation $f_{,t} + v_n f_{,n} - \Phi_{,n}\partial f/\partial v_n = 0$ by 1, then by v_i, then by $v_i v_j$ and integrate over velocity to obtain the Jeans equations of degree 0, 1, and 2. We then eliminate the potential $\Phi_{,i}$ and discard terms proportional to $\sigma_{ijk} \equiv \overline{(v_i - \overline{v_i})(v_j - \overline{v_j})(v_k - \overline{v_k})}$ since these are small compared to σ_{ik} if the velocity dispersion is small. We obtain (e.g. Borderies et al. 1983)

$$\sigma_{ij,t} + \sigma_{ik}\overline{v_j}_{,k} + \sigma_{jk}\overline{v_i}_{,k} + \sigma_{ij,k}\overline{v_k} = 0. \tag{17}$$

We then convert to polar coordinates (R, ϕ) and linearize relative to an axisymmetric state, setting

$$\begin{aligned} \overline{v_R} &= \epsilon\,\mathrm{Re}[u_1(R)e^{i(m\phi-\omega t)}], \\ \overline{v_\phi} &= v_c(R) + \epsilon\,\mathrm{Re}[v_1(R)e^{i(m\phi-\omega t)}], \\ \sigma_{ab} &= \sigma^0_{ab} + \epsilon\,\mathrm{Re}[s_{ab}e^{i(m\phi-\omega t)}], \end{aligned} \tag{18}$$

where $\epsilon \ll 1$, σ^0_{RR} and $\sigma^0_{\phi\phi}$ are related by equation (3), and $\sigma^0_{R\phi} = 0$; for simplicity, we neglect asymmetric drift and set the unperturbed $\overline{v_\phi}$ to the circular speed v_c. For a power-law circular-speed curve $v_c \propto R^\alpha$, we find

$$\ell_v = \epsilon \,\mathrm{Re}\left\{ \frac{2e^{i(m\phi-\omega t)}}{(1-\alpha)\Delta_2} \left[-2(\alpha+1)\Omega u_{1,R} - i\tilde{\omega} v_{1,R} \right.\right. \\ \left.\left. + (\alpha+1)(2\Omega + \tfrac{1}{2}m\tilde{\omega})\frac{u_1}{R} + i\left[2m(\alpha+1)\Omega + \alpha\tilde{\omega}\right]\frac{v_1}{R} \right] \right\} + \mathrm{O}(\epsilon^2), \quad (19)$$

where $\Omega(R) \equiv v_c(R)/R$, $\tilde{\omega} = \omega - m\Omega$, and $\Delta_2 = 8(1+\alpha)\Omega^2 - \tilde{\omega}^2$. The Jeans equations can also be used to relate the perturbed velocities to the perturbing potential, $\epsilon\,\mathrm{Re}\{\psi_1(R)\exp[i(m\phi - \omega t)]\}$,

$$u_1 = \frac{i}{\Delta_1}\left[\tilde{\omega}\psi_{1,R} - 2m\Omega\frac{\psi_1}{R}\right], \quad v_1 = \frac{1}{\Delta_1}\left[\Omega(1+\alpha)\psi_{1,R} - m\tilde{\omega}\frac{\psi_1}{R}\right], \quad (20)$$

where $\Delta_1 = 2(\alpha+1)\Omega^2 - \tilde{\omega}^2$. Equations (19) and (20) are valid so long as the radial scale of the perturbing potential ψ_1 exceeds the typical radial excursion of an orbit $\max[|u_1|, \sigma^{1/2}_{RR}]/\kappa$, where $\kappa = [2(\alpha+1)]^{1/2}\Omega$ is the epicycle frequency.

These expressions simplify considerably in some special cases:

(i) Near a Lindblad resonance ($\Delta_1 \approx 0$) we have $v_1 = -\frac{1}{2}i\tilde{\omega}u_1/\Omega$. Moreover since Δ_1 is small the radial derivatives of u_1 and v_1 will be large. Equation (19) simplifies to

$$\ell_v = -\epsilon\,\mathrm{Re}\left[\frac{u_{1,R}e^{i(m\phi-\omega t)}}{(1-\alpha)\Omega}\right]. \quad (21)$$

Thus radial compression leads to a positive vertex deviation, expansion to a negative deviation. The vertex deviation and radial velocity oscillations are in (anti)phase (*i.e.* they differ in phase by 0 or 180°, so that $|\ell_v|$ is large at azimuths where $|\overline{v_R}|$ is large), while the azimuthal velocity perturbation is in quadrature with the vertex deviation (*i.e.* they differ in phase by 90 or 270°). Notice that the formulae above only hold when we are sufficiently far from the resonance that the local kinematics are not polluted by stars from the opposite side of the resonance.

(ii) Near a corotation resonance ($\tilde{\omega} \approx 0$) equation (19) simplifies to

$$\ell_v = -\frac{\epsilon}{2\Omega(1-\alpha)}\,\mathrm{Re}\left[e^{i(m\phi-\omega t)}\left(u_{1,R} - \frac{u_1}{R} - \frac{imv_1}{R}\right)\right]. \quad (22)$$

This can be rewritten in terms of the Oort constants (13) as

$$\ell_v = -\tfrac{1}{2}C/A + \mathrm{O}(\epsilon^2) = \psi_v + \mathrm{O}(\epsilon^2). \quad (23)$$

Thus, near corotation, the vertex deviation is the same as the offset in the double-sine curve of mean velocity.

(iii) If the oscillation arises from tightly wrapped spiral structure, $\psi_1(R) \propto \exp[i \int k(R) dR]$ with $|kR| \gg 1$, ($k > 0$ for a trailing pattern) then

$$u_1 = -\frac{\tilde{\omega} k \psi_1}{\Delta_1}, \quad v_1 = \frac{ik\Omega(1+\alpha)\psi_1}{\Delta_1}, \quad \ell_v = \epsilon \,\mathrm{Re}\left[\frac{6ik^2\Omega\tilde{\omega}(1+\alpha)}{\Delta_1\Delta_2(1-\alpha)}\psi_1 e^{i(m\phi-\omega t)}\right]. \tag{24}$$

In this case the vertex deviation oscillation is in (anti)phase with the tangential velocity, and in quadrature with the radial velocity and the surface density perturbation (which is $\mu_1 = k\mu_0 u_1/\tilde{\omega}$). Of course, the validity of this formula is limited because it requires that the radial excursion of an orbit $\sigma_{RR}^{1/2}/\kappa$ is less than about $|k^{-1}| \ll R$. If the dispersion exceeds this limit the perturbed forces at different phases of the epicycle tend to average to zero, so that (24) will overestimate the response. A generalization of (24) that is also valid in the case $\sigma_{RR}^{1/2} k/\kappa \gtrsim 1$ was derived by Mayor (1970).

(iv) The kinematic model in the Introduction (eq. 2) yields $\ell_v = (1-q^2)xy/R^2 = -\overline{v_R}/v_0$ to lowest order in $(1-q^2)$. A similar, but slightly more realistic, dynamical model is to assume that the potential of the galaxy is $\Phi(R,\phi) = \frac{1}{2}v_0^2 \ln(x^2 + y^2/q_\Phi^2)$, which for $1 - q_\Phi^2$ small can be decomposed into an axisymmetric potential with circular speed independent of radius ($\alpha = 0$) and a perturbation with $m = 2$, $\omega = 0$, and $\psi_1 = \frac{1}{4}v_0^2(1-q_\Phi^2)$. In this model equations (20) and (19) yield

$$u_1 = \frac{2i\psi_1}{v_0}, \quad v_1 = -\frac{2\psi_1}{v_0}, \quad \ell_v = -4\epsilon \,\mathrm{Re}\left(\frac{i\psi_1 e^{2i\phi}}{v_0^2}\right) = -\frac{2\overline{v_R}}{v_0}. \tag{25}$$

Once again the vertex deviation and radial velocity oscillations are in (anti)phase.

There have been many observational studies of the vertex deviation ℓ_v; for reviews and compilations see Delhaye (1965), Mayor (1972), Wielen (1974), and Jahreiss and Wielen (1983). In general, the stellar populations with the largest velocity dispersions show the smallest vertex deviation. For example, Mayor (1972) lists five groups of disk stars for which the dispersion $\sigma_{RR}^{1/2}$ increases from $17\,\mathrm{km\,s^{-1}}$ to $42\,\mathrm{km\,s^{-1}}$ and the vertex deviation decreases monotonically from $\ell_v = 22°$ to $6°$. Ratnatunga and Upgren (1991) analyzed the kinematics of $\sim$ 800 Vyssotski K and M dwarfs, and found a significant vertex deviation $\ell_v = 12° \pm 4°$ in the cooler ($\sigma_{RR}^{1/2} = 31\,\mathrm{km\,s^{-1}}$) component, but none ($-9° \pm 6°$) in the hotter ($\sigma_{RR}^{1/2} = 54\,\mathrm{km\,s^{-1}}$) component. From proper-motion and parallax measurements towards the South Galactic Pole by Murray et al. (1986), we obtain $\ell_v = -1 \pm 7°$ (assuming that the proper motion errors are isotropic) for the stars between 100 and 300 pc below the Galactic midplane. Erickson's (1975) analysis of the Gliese (1969) catalogue yields a vertex deviation of $9 \pm 3°$ for all stars together.

To reduce the sensitivity of estimates of the dispersion tensor to high-velocity stars, we have computed rank correlation coefficients between v_R and v_ϕ among stars in the Gliese catalog. Bounds on the vertex deviation can be set by repeating this analysis for the (v_R, v_ϕ) distribution rotated through a range of angles and identifying those angles for which the rotated sample shows no significant correlation. We find for the

602 "good" stars (see §2) that v_R and v_ϕ are anticorrelated (*i.e.* that there is a positive vertex deviation) at the 99.5%, 91% and 75% (two-sided) significance level for the $|W| < 6$, 6–15 and $> 15\,\mathrm{km\,s^{-1}}$ subsamples, and values of ℓ_v between 4° and 18°, −1° and 14°, and −7° and 12° are consistent with the data at 95% confidence; the full 1004-star sample gives vertex deviation with > 99.9%, 99.5% and 60% confidence, and intervals of 10° to 20°, 3° to 15°, and −5° to 11°. Although the third bin shows no evidence for any vertex deviation, a deviation of up to 7° for the full sample or 9° for the restricted one cannot be ruled out at the 1-σ level by the observations. In his analysis of the Gliese catalog data, Wielen (1974) coped with the outlier problem by restricting the analysis to stars with $(v_R^2 + (v_\phi - v_c)^2)^{1/2} < 40\,\mathrm{km\,s^{-1}}$, so for the hotter populations a significant fraction of the stars are rejected. Mayor's (1972) clipping of all stars with eccentricity above 0.15 is less severe, but not circularly symmetric in the (v_R, v_ϕ)-plane. The method presented here is a stable alternative that introduces no preferred direction and uses all the data.

To estimate the vertex deviation for the hotter disk stars, we have combined the estimates from Mayor (1972), our analysis of the Gliese (1969) catalog, and Ratnatunga and Upgren (1991), for all classes with radial dispersion $> 30\,\mathrm{km\,s^{-1}}$, computing the weighted mean and likely error according to the prescription of §3.1. We find a weighted mean and likely error

$$\ell_v = 5.5 \pm 4.2°, \tag{26}$$

with external error 2.5° (see Figure 3). For comparison the B&S model predicts $\ell_v = -9.3°$, which differs by 3.5 times the likely error.[3] This is the largest discrepancy between the B&S model and our estimates of local kinematic constants.

The data suggest that the vertex deviation ℓ_v declines from $\sim 20°$ for the coldest stellar populations to a substantially smaller value—possibly near zero—with increasing dispersion. Unfortunately, available data do not exclude the possibility that a non-zero vertex deviation of up to about 10° persists in even the hottest disk stars. Perhaps the HIPPARCOS satellite will provide the data that will settle this important question.

3. 4. THE VELOCITY ELLIPSOID AXIS RATIO

We may derive the perturbations in the dispersions σ_{RR} and $\sigma_{\phi\phi}$ in the same way that we derived the vertex deviation (19):

$$\begin{aligned} \frac{s_{RR}}{\sigma^0_{RR}} &= \frac{1}{\tilde{\omega}} \left[-2iu_{1,R} + ih_\sigma^{-1} u_1 - 2i\Omega(1-\alpha)\ell_1 \right], \\ \frac{s_{\phi\phi}}{\sigma^0_{\phi\phi}} &= \frac{1}{\tilde{\omega}} \left[i(h_\sigma^{-1} - 2R^{-1})u_1 + \frac{2mv_1}{R} + 2i\Omega(1-\alpha)\ell_1 \right], \end{aligned} \tag{27}$$

where ℓ_1 is the complexified vertex deviation and is given by $\ell_v = \epsilon \mathrm{Re}[\ell_1 e^{i(m\phi - \omega t)}]$, and $h_\sigma(R)$ is the local exponential scale length of the unperturbed velocity dispersions

[3] B&S quote a vertex deviation of +10°; however the sign conventions they use do not appear to be consistent. The number quoted here is derived using eq. (19).

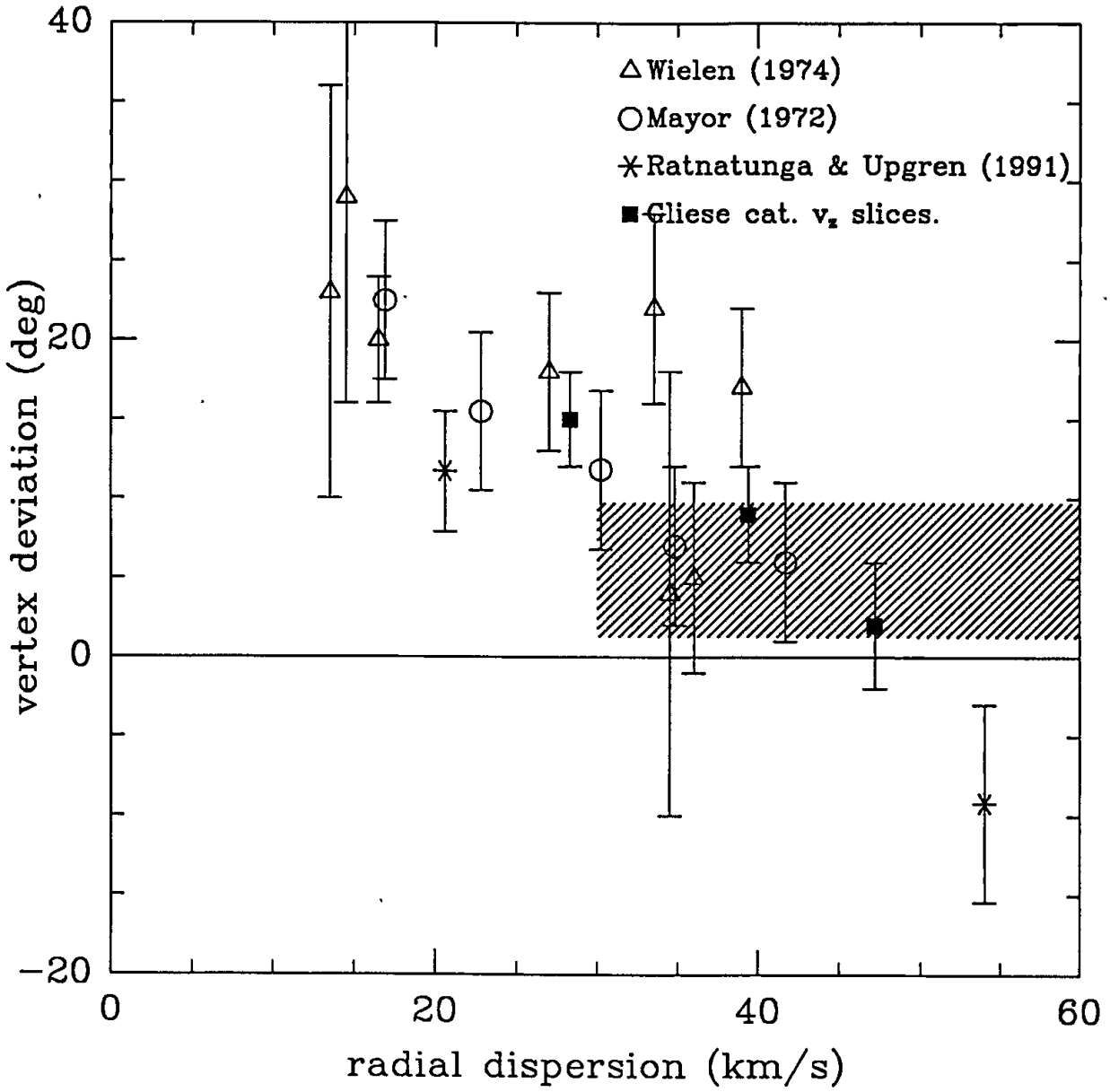

Figure 3. Determinations of the vertex deviation. The shaded region denotes the range allowed by our best estimate and likely error, which are derived from the data with radial dispersion $> 30\,\mathrm{km\,s^{-1}}$. See text for details.

σ^0_{aa} (the ratio of the unperturbed dispersions in radius and azimuth is independent of radius because of equation 3 and our assumption that the rotation curve is a power law). The fractional perturbation in the axis ratio $\sigma_{\phi\phi}/\sigma_{RR}$ is $(s_{\phi\phi}/\sigma^0_{\phi\phi}) - (s_{RR}/\sigma^0_{RR})$. For the special cases (i)–(iv) above, equations (27) simplify as follows:

(i) *Near Lindblad resonance:*

$$\frac{s_{\phi\phi}}{\sigma^0_{\phi\phi}} = \frac{-2iu_{1,R}}{\tilde{\omega}}, \qquad |s_{RR}| \ll s_{\phi\phi}. \tag{28}$$

The oscillations in axis ratio are in quadrature to the oscillations in vertex direction (compare eq. 21).

(ii) *Near corotation resonance:* Both s_{RR} and $s_{\phi\phi}$ are singular at this resonance; however, when near the resonance, we have

$$\frac{s_{RR}}{\sigma^0_{RR}} = \frac{s_{\phi\phi}}{\sigma^0_{\phi\phi}} = \frac{1}{\tilde{\omega}}\left[-iu_{1,R} + i(h_\sigma^{-1} - R^{-1})u_1 + \frac{mv_1}{R}\right]. \tag{29}$$

Thus the axis ratio remains near the axisymmetric value even though the dispersions diverge.

(iii) *Tightly wound spiral:*

$$\frac{s_{RR}}{\sigma^0_{RR}} = -\frac{2k^2\psi_1}{\Delta_2}, \qquad \frac{s_{\phi\phi}}{\sigma^0_{\phi\phi}} = -\frac{12(1+\alpha)k^2\Omega^2\psi_1}{\Delta_1\Delta_2}. \tag{30}$$

The deviation of the axis ratio from its axisymmetric value, the radial velocity, and the density all oscillate in (anti)phase. At radii between the inner and outer Lindblad resonances (where $\Delta_1, \Delta_2 > 0$), the density and the axis ratio maxima coincide.

(iv) *Elliptical disk with flat rotation curve and ellipticity independent of radius:* In this case equations (25) yield

$$\frac{s_{RR}}{\sigma^0_{RR}} = \frac{(R/h_\sigma + 4)\psi_1}{v_0^2}, \qquad \frac{s_{\phi\phi}}{\sigma^0_{\phi\phi}} = \frac{(R/h_\sigma - 2)\psi_1}{v_0^2}. \tag{31}$$

The oscillations of the axis ratio are in quadrature with oscillations in vertex direction but in (anti)phase with oscillations in azimuthal velocity.

3. 5. IMPLICATIONS

Clearly the existing data on local kinematics do not provide accurate estimates for the vertex deviation and its variation with dispersion. The coldest populations show large vertex deviations, which probably reflect incomplete mixing because of their young ages. For the older, hotter populations the following two models are both consistent with the local data:

(i) The vertex deviation ℓ_v is independent of dispersion and equal to about $5° \pm 5°$. The absence of dispersion dependence in both ℓ_v and $\overline{v_R}$ then suggests that both

arise from a large-scale oscillation. In this case, however, a vertex deviation as large as 5–10° is difficult to reconcile with other evidence: (a) If the oscillation is caused by a non-axisymmetric halo (as in case [iv] above) then $\ell_v = -2\overline{v_R}/v_c$ so we expect $\overline{v_R} \approx -10$ to $-20\,\mathrm{km\,s^{-1}}$. There is no evidence for such a rapid inward motion in the data discussed in §3.2, which suggest near-zero or outward motion of the LSR. (b) If we are near a Lindblad resonance (case [i]) then $\overline{v_{R,R}} = -\Omega\ell_v \simeq -2$ to $-5\,\mathrm{km\,s^{-1}\,kpc^{-1}}$. This violates the limits $|\overline{v_{R,R}}| < 2\,\mathrm{km\,s^{-1}\,kpc^{-1}}$ obtained in §3.1 from limits on Oort's C and K constants. (c) Near a corotation resonance, $\ell_v = \psi_v$ which is less than 1° according to §3.1.

(ii) The vertex deviation declines with dispersion, from $\approx 10°$ for young but well-mixed populations to near zero for older, hotter disk populations. The decline suggests that the vertex deviation is caused by a small-scale oscillation, perhaps a nearby spiral arm or other mass concentration (as in case [iii]) above (see Wielen 1979 for a general discussion of the effects of spiral structure on local kinematics). If this is so, we can attempt to constrain our position with respect to the arm from the observed kinematics. Figure 4 shows the vertex deviation and perturbed streaming motions in the region between the inner and outer Lindblad resonance of a trailing ($m = 2$, $k = 20/R$, corotation at $R = 1$) spiral in a galaxy with a flat rotation curve. Contours of constant positive (negative) vertex deviation are plotted as solid (dashed) lines, and the potential minima (the centres of the spiral arms) are marked as crosses. Then, if the Sun lies outside the corotation radius, the observed positive vertex deviation requires us to be just outside (leading) the arm (*i.e.* $kR - kR_a \in [0, \pi]$ at fixed azimuth, where R_a is the radius at the centre of the arm); if inside corotation, we would have to lie just inside (trailing) the arm instead. To obtain a further constraint, we use the line-of-sight velocity map of OB stars, compiled by Burton and Bania (1974). The most striking feature on this map is a region of compression along the line of sight towards $\ell = 120°$, at a distance of $\sim 2\,\mathrm{kpc}$: comparing with Figure 4 once again, we see that this would only be observed from the leading edge of an arm. Thus, we conclude that if the vertex deviation and the OB star peculiar velocities are a result of a tightly-wound spiral perturbation, the Sun must lie just outside an arm, and outside the corotation circle. The general features of the data can be reproduced in such a model. (Burton and Bania's fit of the velocity field to a trailing spiral density wave also placed the Sun on the outside edge of an arm: but because the adopted corotation radius for their model is $\sim 20\,\mathrm{kpc}$, the vertex deviation predicted by their model is negative.)

Thus we believe that the vertex deviation is mostly due to small-scale rather than large-scale oscillations (option [ii] rather than [i]), although it would be reassuring to have better data on the deviation so that we could detect its dispersion dependence with more confidence.

Oscillations in the axis ratio of the velocity ellipsoid may explain the $\sim 30\%$ discrepancy between the predicted and observed ratios for a flat rotation curve (§2). For example, in case (iv) above, oscillations with zero pattern speed and constant ellipticity, the amplitude of the fractional oscillations in the axis ratio is $\frac{3}{2}$ times the amplitude

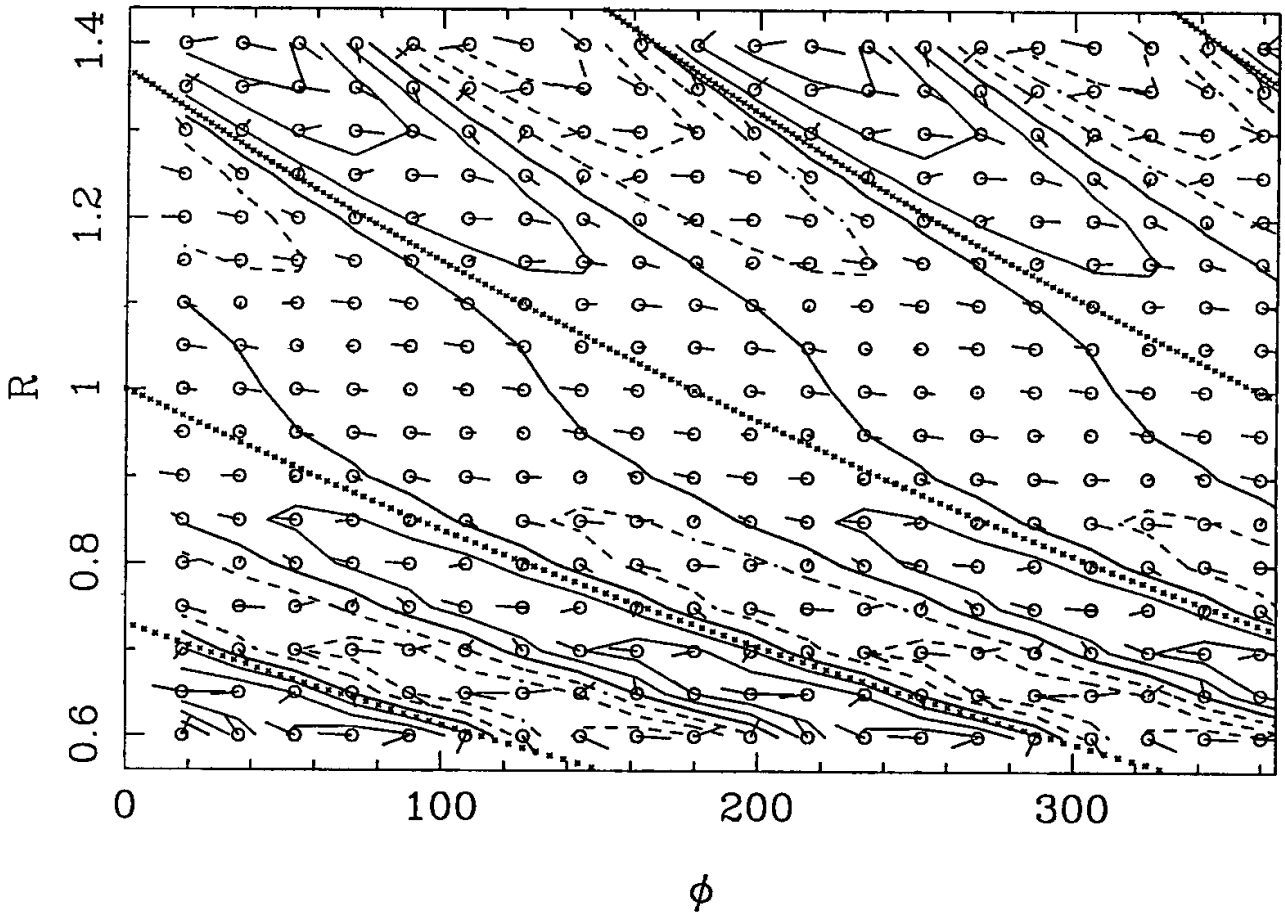

Figure 4. Streaming motions and vertex deviation in a tightly-wound spiral pattern. The unperturbed rotation curve is flat with circular speed $v_c = 1$. The potential perturbation is the real part of $0.002\exp[20i\ln R + 2i(\phi - t)]$; potential minima are marked by x's. Streaming motions are marked by small vectors whose tails are denoted by circles; at multiples of 5°, contours of constant vertex deviation are marked by solid lines (positive deviation) or dashed lines (negative deviation).

of the oscillations in the vertex longitude, and the vertex oscillates in quadrature with the axis ratio. Thus if the Sun is close to a symmetry axis of the elliptical distortion in the disk, we would expect a small vertex deviation and a large deviation in axis ratio (because the observed axis ratio is smaller than the predicted one, the Sun must be near the minor axis of the ellipse). An appealing aspect of this explanation is that the fractional change in axis ratio is $3(\overline{v_\phi} - v_c)$, so a 30% change in axis ratio requires only a 10% oscillation in azimuthal velocity. It is also interesting that the Sun appears to lie near the line of nodes of the Galaxy's warp. In models in which the warp is the result of a mismatch between the symmetry planes of the disk and a non-spherical halo (Toomre

1983, Dekel and Shlosman 1983, Sparke and Casertano 1988), the line of nodes is the major (minor) axis of the halo potential in the disk plane if the halo is oblate (prolate). Thus it would not be surprising if the Sun were near the symmetry axis of an elliptical distortion, which is consistent with the small vertex deviation and the near-zero values for the Oort constants C and K.

Of course, the velocity ellipsoid does not exhaust the information available in the local velocity distribution. For example, we argued in §2 that the distributions of v_R and v_z should be symmetric about zero. We have tested the symmetry of the v-distributions of the Gliese catalogue by using the Kolmogorov-Smirnov test to compare the distribution and its reflection about a hypothesized centre of symmetry. For the 602- and 1004-star samples as well as the slices in $|v_z|$ mentioned above, the only asymmetry detected at better than 90% significance is in the v_ϕ distribution: this shows very significant ($> 99\%$) asymmetry about the mean, as expected, and the v_ϕ-distributions of the $|v_z| > 15\,\mathrm{km\,s^{-1}}$ bins are also asymmetric about the median at better than 95%. However, Jahreiss and Wielen (1983) point out that there is a noticeable asymmetry in the v_R distribution of the McCormick K and M dwarfs. The interpretation and significance of this asymmetry is unclear.

3. 6. MIXING

Star formation does not occur at uniform rates across the Galactic disk. Spatial and temporal variations in the star formation rate are gradually washed out as stars travel at different velocities away from their birthplaces ("phase mixing"). To what extent do the stars of the solar neighbourhood form a well-mixed system? This question is fundamental to any interpretation of the kinematics of the solar neighbourhood, since many of the predictions we have made are only valid for a well-mixed population.

Irregularities in the Galactic gravitational field heat stellar populations as they age (Wielen 1977, Jenkins and Binney 1990). Thus, if vertex deviation is only present in the kinematically cooler (and therefore younger) stars, there are at least two possible explanations: the deviation could be caused by a short-wavelength oscillation on a well-mixed population, or by incomplete mixing of the youngest stars in an otherwise unperturbed disk. Here we estimate the mixing timescale to assess the second possibility. For previous discussions, see Woolley (1965) and Mayor (1972).

Consider the simplified case of a group of stars that are born simultaneously in a small patch of phase space of size $\Delta \mathbf{v}_0$ in velocity and $\Delta \mathbf{x}_0$ in space. Assume further that once born, these stars respond only to the large-scale gravitational field of the Galaxy, and not to each other, so that we can study their orbits separately.

In the epicycle approximation, the orbit of a star initially at (R_0, ϕ_0) with velocity

$(v_{R0}, v_c(R_0) + v_{p0})$ is

$$\begin{aligned} R(t) =& R_0 + \frac{2\Omega_e}{\kappa_e^2} v_{p0}(1 - \cos\kappa_e t) + \frac{v_{R0}}{\kappa_e}\sin\kappa_e t \\ \phi(t) =& \phi_0 + \Omega_e t + \frac{2\Omega_e}{R_0\kappa_e^2} v_{R0}(\cos\kappa_e t - 1) + \frac{4\Omega_e^2}{R_0\kappa_e^3} v_{p0}\sin\kappa_e t \\ v_R(t) =& v_{R0}\cos\kappa_e t + \frac{2\Omega_e}{\kappa_e} v_{p0}\sin\kappa_e t \\ v_\phi(t) =& v_c(R_0) + v_{p0}\left[1 + \frac{2\Omega_e^2}{\kappa_e^2}(\cos\kappa_e t - 1)\right] - \frac{\Omega_e}{\kappa_e} v_{R0}\sin\kappa_e t. \end{aligned} \tag{32}$$

In these formulae Ω_e and κ_e are the usual azimuthal and epicycle frequencies evaluated at the star's guiding centre or mean radius R_e.

We first ask how such an unbound group of stars would look to a local observer. Equations (32) show that while R, v_R and v_ϕ oscillate about a fixed mean, the azimuth ϕ of the group is sheared out at the rate proportional to $|\Delta\Omega_e|$, the spread in azimuthal frequencies of the guiding centres. Thus at large times, all of the stars in a given azimuthal interval $\Delta\phi \ll 1$ would have the same guiding centre radius R_e (we neglect the possibility that the leading stars in the group may lap the trailing stars). The first of equations (32) shows that the guiding centre radius is related to the initial radius and velocity by

$$R_e = R_0 + \frac{2\Omega}{\kappa^2} v_{p0}, \tag{33}$$

where to sufficient accuracy we have replaced Ω_e, κ_e by Ω, κ, the frequencies evaluated at the present radius. Since there is nothing special about the initial time, this relation also holds if the initial radius and velocity are replaced by the present radius and velocity. Thus for $\Omega t \gg 1$ the stars from the group that are visible in a given azimuthal interval occupy a narrow band in phase space given by

$$R + \frac{2\Omega}{\kappa^2} v_p \simeq \text{constant}; \tag{34}$$

that is, the signature of incomplete mixing is streaks in $R - v_p$ space.

The solar neighbourhood is well-mixed if many such streaks are present. To estimate the mixing efficiency, let us assume that all stars of a particular type X are born in clusters containing N_X such stars, that these clusters are formed at a uniform rate p per unit time and per unit area of the disk, and that the clusters disrupt soon after forming into unbound groups of stars with typical internal velocities and sizes Δv and ΔR. We assume, as is probably the case, that the clusters' velocities are much larger than their sizes, $\Delta v/v_c \gg \Delta R/R_0$ or $\Delta v \gg 0.02\,\mathrm{km\,s^{-1}}(\Delta R/1\,\mathrm{pc})$. The group shears out into a stream of azimuthal extent $\Delta\Omega_e t \approx (\Delta v/v_c)\Omega t$, and of radial extent $(\Delta v/v_c)R$ (we do not distinguish κ from Ω at this level of approximation). Thus the area of a stream of age t is $A(t) \approx R^2(\Delta v/v_c)^2\Omega t$, and the number of streams overlapping at a given position with age $< t$ is

$$n(t) = p\int_0^t A(t)dt \approx pR^2(\Delta v/v_c)^2\Omega t^2. \tag{35}$$

The youngest and hence highest density stream visible in the solar neighbourhood will have age t_1 such that $n(t_1) \approx 1$, and a surface number density of stars $\Sigma_1 = N_X/A(t_1)$. The total surface number density of X-stars is $\Sigma_X = pN_X\tau_X$, where τ_X is either the age of the Galaxy or the lifetime of the stars in question (whichever is shorter), so we may eliminate p to obtain

$$\frac{\Sigma_1}{\Sigma_X} \approx \frac{v_c}{\Delta v}\left(\frac{N_X}{\Sigma_X R^2 \Omega \tau_X}\right)^{1/2}. \tag{36}$$

Also, since $p = \Sigma/(N\tau)$ is the same for all stellar types, we have in particular $N_X/N_* = (\Sigma_X\tau_*)/(\Sigma_*\tau_X)$ where the asterisk subscript denotes the entire stellar disk population: for our purposes it is adequate to set $\tau_* = \tau_D$, the age of the Galactic disk. Then, using plausible parameters, we obtain

$$\frac{\Sigma_1}{\Sigma_X} \approx 0.007\left(\frac{5\,\mathrm{km\,s^{-1}}}{\Delta v}\frac{1\,\mathrm{Gyr}}{\tau_X}\right)\left(\frac{N_*}{300}\frac{\tau_D}{10\,\mathrm{Gyr}}\frac{50\,\mathrm{pc^{-2}}}{\Sigma_*}\right)^{1/2}; \tag{37}$$

the ratio indicates the fraction of solar neighbourhood stars in the strongest stream.

For early A stars, with main-sequence lifetimes of $\tau_A \approx 2 \times 10^8$ yr, we expect that roughly 3.5% are in the strongest stream if these parameter values are correct. In this case the observed structure in the early A star velocity distribution (see Eggen 1965, Figure 2) is not likely to be the result of incomplete mixing. However, if only some fraction f_M of clusters form stars as massive as A stars, which could happen for example if the IMF depends on star forming environment, then the stream strength is increased by a factor $f_M^{-1/2}$; so equation (37) is likely to underestimate the velocity clumping.

Are stellar "moving groups" (Eggen 1965) such shredded clusters? It is quite possible that f_M and the parameters in equation (37) can be stretched enough so that the observed clumpiness in the distribution of A stars can be reconciled with such a model. One prediction of this model, already pointed out by Woolley (1965), is a narrowing of the v_ϕ-, but not the v_R-distribution of each stream with age: after 0.5 Gyr, the tangential velocity width should amount to no more than $\sim 1\,\mathrm{km\,s^{-1}}$ (though the shear expressed in eq. 34 will project to add some further width if the radius range sampled is nonnegligible). In addition, the number of stars in each group should decrease as t^{-1}, *i.e.* the density of stars in the (v_R, v_ϕ) plane should be roughly the same within all groups (conservation of phase-space density). While we have made no detailed comparison, the A star distribution does appear to show some of these features to the eye. Further support for the notion that the moving groups are physically associated stars, rather than chance coincidences, comes from detailed photometric studies of stars with the moving group kinematics, which suggest common metallicities and ages for the stars in any one stream (a review of this subject is presented in Eggen 1989).

4. The effect of oscillations on large-scale kinematics

The strongest evidence for large-scale oscillations is likely to be found in the kinematics of distant tracers. The difficulty is to find a suitable tracer: a member of the disk population that is visible across the Galaxy and whose distance and velocity can be determined reliably.

There are major surveys of the region outside the solar radius ($R_\odot < R < 2R_\odot$) in both carbon stars (Aaronson et al. 1989, 1990) and HII regions (Brand 1986; Fich et al. 1989). There is no strong evidence of deviations from axisymmetry in either survey, although detailed comparisons with the B&S or other models are not available. Part of the problem is that the B&S model has a Lindblad resonance at $1.5R_\odot$. Orbit crossing is inevitable in the vicinity of this resonance; the detailed behaviour of the gas will then depend on its effective viscosity, and collisionless populations will exhibit an enhanced velocity dispersion rather than oscillations in mean velocity. Thus the theoretical prediction is uncertain and its observational consequences are difficult to detect. This problem is artificially minimized in the B&S model by smoothly truncating the quadrupole component of the potential to zero before the resonance radius.

In the K giant survey of Lewis and Freeman (1989), the radial velocities along the line of sight near the anticentre appear to deviate systematically from the LSR motion: at $R = 1.5R_\odot$, $1.75R_\odot$ and $2.1R_\odot$, they find $\overline{v_R}(R) - v_{R,\mathrm{LSR}} = 13.0 \pm 4.2\,\mathrm{km\,s^{-1}}$, $16.1 \pm 4.6\,\mathrm{km\,s^{-1}}$ and $5.7 \pm 4.5\,\mathrm{km\,s^{-1}}$.[4] If the outer regions of the Galaxy are not oscillating, the only effect we could see in the velocities at these radii would be the reflex of the LSR motion: then these stellar data suggest $v_{R,\mathrm{LSR}} = -11.6 \pm 2.6\,\mathrm{km\,s^{-1}}$ (an inward motion), opposite to the outward motion suggested by B&S. It would be very interesting to confirm this result with different samples.

If the Galaxy has a single pattern speed (*i.e.*, if there is some frame rotating at Ω_p in which the density and velocity distributions are stationary), then one can derive from the continuity equation an integral constraint on the line-of-sight kinematics of the tracers in any distance-limited survey: let $\Sigma(r,\ell)$ be the surface density of the tracer at distance r (from the Sun) and longitude ℓ, and let $g(r)$ be the probability that an object at distance r is included in the survey (the selection function). We define, for any observable quantity $f(r,\ell)$, $\langle f\rangle = \int_0^\infty dr \int_0^{2\pi} d\ell\, \Sigma(r,l) g(r) f(r,\ell)$. Then

$$\langle v_{\mathrm{rad}}\rangle + (v_{\phi,\odot} - \Omega_p R_\odot)\langle \sin\ell\rangle = v_{R,\mathrm{LSR}}\langle\cos\ell\rangle. \tag{38}$$

This formula requires uniform completeness in ℓ, that is, the selection function must be independent of longitude. Using the Galactic HI distribution, eq. (38) yields $v_{R,\mathrm{LSR}} = 8\,\mathrm{km\,s^{-1}}$ if $\Omega_p = 0$ (a reasonable lower limit), and $v_{R,\mathrm{LSR}} = -4\,\mathrm{km\,s^{-1}}$ for a perturbation that corotates at the sun. Estimating the error on this determination is very difficult. Ideally we should apply the same method to different tracers, but unfortunately there are few extensive data sets with the required ℓ-coverage and uniform completeness.

[4] It is interesting that these deviations are opposite to the tail towards negative v_{rad} seen in the HI line profile towards the anticentre.

4. 1. GAS KINEMATICS

The surface density of HI falls rapidly at large radii and hence the "edge" of the HI distribution (as given, say, by the 1 K contour of brightness temperature) can be used to trace the line-of-sight velocity of a streamline as a function of longitude. Spiral arms are weak or non-existent well outside $R_\odot$ so deviations from axisymmetry are more likely caused by large-scale oscillations. The following analysis of the effects of oscillations on a streamline follows Kuijken (1991).

Let the velocity field of the HI be $v_R(R,\phi)\hat{\mathbf{e}}_R + v_\phi(R,\phi)\hat{\mathbf{e}}_\phi$, where $\phi = 0$ is the line from the Galactic centre to the Sun (recall that ϕ increases counterclockwise when viewed from the South Galactic Pole). If the LSR (coordinates $R = R_\odot$, $\phi = 0$) follows the velocity field of the HI, then the line-of-sight velocity of HI at radius R and longitude ℓ is

$$v_{\rm rad} = v_\phi(R,\phi)(R_\odot/R)\sin\ell - v_{\phi,\odot}\sin\ell - v_R(R,\phi)\cos(\phi+\ell) + v_{R,\odot}\cos\ell, \qquad (39)$$

where $v_{\phi,\odot} = v_\phi(R_\odot, 0)$ is the azimuthal velocity of the LSR, with a similar definition for $v_{R,\odot}$, and the angles ϕ and ℓ are related by $R\sin(\phi+\ell) = R_\odot\sin\ell$.

Now assume that oscillations are of order $\epsilon \ll 1$, so we may write

$$v_R = \epsilon\alpha(R)\sin[m\phi - \zeta(t)], \qquad v_\phi = v_c(R) + \epsilon\beta(R)\cos[m\phi - \zeta(t)], \qquad (40)$$

where the functions α and β can be deduced from equation (20) for a given potential perturbation and $d\zeta(t)/dt = \omega$ is the frequency of the oscillation. We evaluate the line-of-sight velocity along a streamline with mean radius R_s to O(ϵ). To account for variations in v_c with radius we need to know the difference between the instantaneous and mean radius of the streamline, which is $R - R_s = \epsilon\gamma(R_s)\cos(m\phi - \zeta)$ where $\gamma = \alpha/\tilde{\omega} = \alpha/(\omega - m\Omega)$ and $\Omega(R) = v_c(R)/R$. Thus

$$\begin{aligned} v_{\rm rad} =& R_\odot(\Omega_s - \Omega_\odot)\sin\ell + \epsilon\Big\{\Big[\beta_s\frac{R_\odot}{R_s} + \gamma_s(\Omega_{,R})_s R_\odot\Big]\sin\ell\cos(m\phi-\zeta) \\ & - \alpha_s\cos(\phi+\ell)\sin(m\phi-\zeta) - \beta_\odot\sin\ell\cos\zeta - \alpha_\odot\cos\ell\sin\zeta\Big\}, \end{aligned} \qquad (41)$$

where subscripts correspond to the radii where the functions are to be evaluated. Following B&S, we note that the term independent of ϵ is odd in ℓ, so we eliminate this term by forming

$$\begin{aligned} \Delta v_{\rm edge} =& v_{\rm rad}(\ell) + v_{\rm rad}(-\ell) \\ =& 2\epsilon\sin\zeta\Big\{\Big[\beta_s\frac{R_\odot}{R_s} + \gamma_s(\Omega_{,R})_s R_\odot\Big]\sin\ell\sin m\phi + \alpha_s\cos(\phi+\ell)\cos m\phi - \alpha_\odot\cos\ell\Big\}. \end{aligned} \qquad (42)$$

Note that if $\zeta = 0$ then $\Delta v_{\rm edge} = 0$; this case corresponds to the model in the Introduction in which the Sun lies on a symmetry axis so that oscillations are difficult to

detect in the velocity field. For distant gas, $R_s \gg R_\odot$, we have $R_\odot(d\Omega/dR)_s \to 0$ and $\phi \simeq \pi - \ell$ so that

$$\Delta v_{\rm edge} = 2\epsilon \sin\zeta \left[\alpha_s(-1)^{m+1}\cos m\ell - \alpha_\odot \cos\ell\right]. \tag{43}$$

Thus we conclude that (i) the signature of radial motion of the LSR is a $\cos\ell$ dependence in $\Delta v_{\rm edge}$; (ii) excess azimuthal motion of the LSR is undetectable in $\Delta v_{\rm edge}$; (iii) oscillations in the distant streamline with azimuthal wavenumber m cause oscillations in $\Delta v_{\rm edge}$ as a function of longitude with the same wavenumber.

B&S analyze HI surveys and show that $\Delta v_{\rm edge}$ varies approximately as $\cos\ell$, with an amplitude of $25 - 30\,{\rm km\,s^{-1}}$. The analysis above shows that this variation could result from either (i) outward motion of the LSR at about $15\,{\rm km\,s^{-1}}$ (the interpretation favoured by B&S); or (ii) an $m = 1$ oscillation in the outer Galaxy and no radial velocity for the LSR (Kuijken 1991). In either interpretation, $\Delta v_{\rm edge}$ should be zero at $\ell = 90°$; the actual zero lies at $\ell = 105°$, consistent within the uncertainties.

Other evidence from HI kinematics does not clearly distinguish these two models. B&S point out that the HI at $\ell = 180°$, where the contribution from rotation to the line-of-sight velocity is zero, is mostly at negative velocities, consistent with an outward motion of the LSR that is not shared by more distant gas. However, similar behaviour is expected for an $m = 1$ oscillation. In addition, Kuijken (1991) argues that the B&S model contains a Lindblad resonance outside the solar circle; this implies that $\overline{v_R}(R)$ reverses in sign and then declines for $R > R_\odot$, which should be reflected in a sharp edge to the brightness temperature profile in velocity space rather than the observed extended wing. However, hydrodynamical simulations are needed to predict accurately the behaviour of the gas near the resonance.

Kuijken (1991) shows that the gradient of line-of-sight velocity with brightness temperature is approximately odd around $\ell = 90°$ (although the plots are quite noisy); this is evidence for an $m = 1$ oscillation since motion of the LSR would not produce this asymmetry.

B&S argue that the integrated brightness temperature also shows asymmetries in longitude that are consistent with outward motion of the LSR but not with an $m = 1$ oscillation. However, because the HI surface density falls rapidly with distance the asymmetries are probably dominated by local gas, which participates in spiral structure (the dominance of nearby gas is enhanced because B&S integrate over all latitudes $|b| \le 10°$, so their beamwidth exceeds the HI scaleheight except near the Sun).

Differences in the HI terminal velocity curves between the northern ($0 < \ell < 90°$) and southern ($360 > \ell > 270°$) hemispheres were first detected by Kerr (1962), who postulated an outward LSR velocity $v_{R,\rm LSR} = 7\,{\rm km\,s^{-1}}$ to account for the difference. The difference $\Delta v_{\rm term} = v_{\rm term}(\ell) + v_{\rm term}(-\ell)$ is plotted by B&S and reaches a maximum amplitude of $13\,{\rm km\,s^{-1}}$. The terminal velocity asymmetry is less useful as a discriminant for oscillation models, partly because the amplitude is small (the relevant physical quantity is of course $\frac{1}{2}\Delta v_{\rm term}$, which is only 3% of the circular speed) and partly because much of the asymmetry may be caused by spiral structure. To lowest order in ϵ,

$$\Delta v_{\rm term} = 2\epsilon \sin\zeta \left[\beta_t \sin m(90° - |\ell|) - \alpha_\odot \cos\ell\right], \tag{44}$$

where the subscript t means that the coefficient is evaluated at $R_t \equiv R_\odot |\sin \ell|$. B&S fit their model to $\Delta v_{\rm term}$ to determine the pattern speed of the oscillation; however, even the best-fit pattern speed does not substantially improve the fit in comparison to the prediction $\Delta v_{\rm term} = 0$ for an axisymmetric, stationary galaxy. The same is true of other low-m, large-scale oscillations. Only a high m or a short radial wavelength perturbation can reproduce the details of the terminal velocity differences.

The plane of maximum HI density is warped. The warp is nicely symmetric out to about $1.5R_\odot$ (it can be modelled well as a superposition of concentric circular mutually tilted planar rings), with the line of nodes nearly along the line from the Galactic centre to the Sun (Burton and te Lintel Hekkert 1986). Beyond this radius the symmetry is lost: towards $l = 90°$ the warp angle keeps on increasing, but towards $l = 270°$ it decreases, bending back towards the plane of the inner disk. The gas density in the region of greatest warping is very small.

No revision in the kinematic distance scale can remove the asymmetry in shape between the two sides of the warp, and this asymmetry is difficult to reproduce with gas that follows closed orbits in any simple potential. Thus there is a strong possibility that the outermost gas (beyond about $1.5R_\odot$, say) is not on closed orbits with well-defined, discrete oscillation frequencies. For this reason, any conclusions about the existence or nature of oscillations drawn from the kinematics of distant gas are suspect. Efforts to find a pattern speed for the large-scale oscillations of the Galaxy may be no more fruitful than efforts to find the pattern speed of spiral structure in many external galaxies.

5. Oscillations in other galaxies

The detectability of large-scale oscillations in other disk galaxies depends strongly on the azimuthal wavenumber. We first consider $m = 2$ oscillations, which distort an azimuthally symmetric disk into a disk whose isophotes and streamlines are concentric ellipses. The strongest instabilities in dynamical models of disk galaxies usually have $m = 2$ (Toomre 1977, Sellwood 1985); in addition, both the bars found at the centres of many disks and the two-armed "grand design" spirals found in some galaxies are mainly $m = 2$ oscillations. We concentrate here on elliptical distortions with aligned major axes since these are much harder to detect than spiral distortions.

If disks are azimuthally symmetric, they appear circular when viewed face-on, while elliptical disks only appear circular when the line of sight and the disk axis make an angle of $\cos^{-1} q$ and the minor axis is normal to both. Thus for randomly oriented elliptical disks the distribution of apparent axis ratios Q depends on the distribution of true axis ratios q. Binney and de Vaucouleurs (1981) have examined the Q-distribution of $\sim 10^3$ spiral galaxies and find that for several Hubble types the distribution cannot be fit by randomly oriented, flat, circular disks: there are too few apparently round galaxies ($Q \approx 1$). They find that flat elliptical disks with $q = 0.9$ provide substantially better fits, but that a substantial population with larger ellipticities is incompatible with the data. Grosbol (1985) digitized the images of ~ 600 disk galaxies from Palomar Sky Survey plates and also finds too few round disk galaxies. Athanassoula et al. (1982)

have also derived an average axis ratio $q \simeq 0.9$ from the distribution of apparent axis ratios of outer rings and 25^m isophotes.

A related test is to identify face-on disks from narrow HI line widths and then to measure the ellipticities of these disks (more elaborately, we may compare the "photometric inclination" $i_p = \cos^{-1} Q$ determined from the assumption that the disk is flat and circular with the "Fisher-Tully" inclination $i_{FT} = \sin^{-1}(\Delta v/\Delta v_{FT})$ where Δv is the HI velocity width and Δv_{FT} is the width predicted by the Fisher-Tully relation). In a sample of 212 disk galaxies with apparent axis ratio $Q > 0.87$, Lewis (1987) found $\sim 20\%$ with Fisher-Tully inclinations that would imply apparent axis ratios < 0.8 if the galaxies were round and flat. Though this result should be treated with reserve since the photometry is crude and there are possible systematic errors (e.g. warps may influence the HI widths) it again suggests that intrinsic axis ratios $q \simeq 0.9$ may be common in disk galaxies.

Kent (1990) has carried out a more careful study of a smaller sample of disk galaxies. He has examined 32 galaxies whose Fisher-Tully inclinations imply that the apparent axis ratio Q should exceed 0.9 if the disks are flat and circular; in fact, imaging shows that the distribution of Q is roughly uniform between 0.75 and 1, implying a mean intrinsic axial ratio of about 0.9.

Kormendy (1979, 1982) argues that many elliptical disk galaxies can be identified photometrically, because they contain two or more elliptical disks or rings with different apparent axis ratios or position angles, implying that not all can be round and coplanar. These features are not associated with the warps seen in edge-on disks because they appear at relatively high surface brightnesses, corresponding to radii where edge-on disks are known to be flat. He derives a mean intrinsic axis ratio $q = 0.76$ for the outer rings; however, the ring may be associated with a resonance, so its ellipticity may not reflect the overall ellipticity of the outer disk.

More recently, Bertola et al. (1991) have studied the misalignment between disk and bulge major axes in a sample of 32 "bar-free" nearby spirals. If all this misalignment is due to the disks, they deduce a typical disk axis ratio of 0.85, although the actual value is probably higher since at least some of the misalignment is due to the bulges' triaxiality.

Oscillations can also be detected by analyzing the constant-velocity contours in HI maps (Binney 1978; see also Bosma 1981). Both warped disks and elliptical disks distort the constant-velocity contour field away from the simple shape expected for a flat, axisymmetric disk. The presence of warps in disk galaxies is easier to establish than the presence of elliptical disks, because warped edge-on galaxies are unmistakable, while elliptical disks are difficult to detect unambiguously at any orientation. Nevertheless, the common practice of fitting HI maps to models consisting of inclined, circular rings is suspect, since flat, elliptical rings may often be a better approximation. Staveley-Smith et al. (1990) show that warped and elliptical disks provide equally good fits to the HI velocity field of the irregular galaxy Michigan 160.

Elliptical disks arise naturally if they are embedded in triaxial dark halos (Binney 1978), and we may use models of halo formation to predict disk axial ratios. Dubinski

and Carlberg (1991) have carried out N-body simulations of the formation of halos from cold dark matter, which follow the collapse of individual proto-halos with high spatial resolution (softening length $< 1h^{-1}$ kpc, particle mass $< 10^8 h^{-1}\,M_\odot$, where h is the Hubble constant in units of $100\,\mathrm{km\,s^{-1}Mpc^{-1}}$). They find that the density profiles of the halos can be fit to a Hernquist (1990) model, $\rho = Ca^{-1}(a+a_s)^{-3}$, where C is a constant, $a^2 = x^2 + y^2/q_1^2 + z^2/q_2^2$ and q_1, q_2 are the axis ratios, $1 > q_1 > q_2$. The typical scaling radius $a_s = 22h^{-1}$ kpc. In the limit $R \ll a_s$ the circular speed of the halo is proportional to $R^{1/2}$, so for consistency with the observed flat rotation curves of disks the disk mass must contribute substantially to the rotation speed; we assume that this extra mass is axisymmetric so the only non-axisymmetric potential arises from the halo. If the axial ratios are near unity then the non-axisymmetric component of the potential in one of the principal planes is $\Phi(R,\phi) = \mathrm{Re}(\psi_1 \exp 2i\phi)$, where $\psi_1(R) = \frac{1}{4}\pi G C a_s^{-2}\delta g(R/a)$, R and ϕ are the radius and azimuthal angle, $g(x)$ is a function that we shall not bother to write down but that is normalized so that $g(x) \to x$ as $x \to 0$, and $\delta = 1 - q_1^2$ or $1-(q_2/q_1)^2$ depending on whether the normal to the principal plane is the long axis or the short axis (motion around the intermediate axis is unstable).

The resulting velocity perturbations to the disk material are described by equations (20) in the linear approximation. If the density gradients in the outer regions of the unperturbed disk are large, the ellipticity of the disk will be that of its outermost orbits (*i.e.* isophotes coincide with streamlines). Since the stars follow orbits described by $dR(t)/dt = \mathrm{Re}[u_1 \exp(im\phi(t) - i\omega t)] \simeq \mathrm{Re}[u_1 \exp(-i\tilde{\omega}t)]$, the corresponding axis ratio is $q = 1 - d$ where $d \ll 1$ is given by $d = 2|u_1/R\tilde{\omega}|$. Specializing equations (20) to $m = 2$, a flat disk rotation curve ($\alpha = 0$, circular speed v_c) and $\omega = 0$ since the halo is non-rotating, we obtain $d = \pi G C\delta[2g(x) + xg'(x)]/(4a_s^2 v_c^2)$ where $x = R/a_s$.

The maximum circular speed of the halo is given by $v_{\max}^2 = \frac{1}{2}\pi GC/a_s^2$ so the axis ratio of the disk is given by

$$\begin{aligned} d &= \tfrac{1}{2}\delta\frac{v_{\max}^2}{v_c^2}[2g(x) + xg'(x)]_{x=R/a_s} \\ &= \delta\frac{v_{\max}^2}{v_c^2}\left[6\frac{\log(1+x)}{x^3} - \frac{6+15x+11x^2}{x^2(1+x)^3}\right]_{x=R/a_s}. \end{aligned} \tag{45}$$

Assuming $v_{\max} \simeq v_c$, and setting $R \simeq 0.5a_s$, we find $d = 0.2\delta$ (in fact, the distortion is maximized at $R = 0.45a_s$ where $d = 0.204\delta$). The typical values of δ found by Dubinski and Carlberg (1991) are in the range $0.4-0.7$ (axis ratios $q_1 = 0.56$, $q_2 = 0.42$), yielding disk axis ratios in the range 0.92 to 0.86, consistent with the ratio 0.9 suggested by the observations of external galaxies. In our own Galaxy, at $R \sim 2R_\odot$, the ellipticities of the orbits should be $\sim 0.16\delta$, corresponding to radial velocity oscillation amplitudes $\epsilon\alpha$ of 0.06–$0.11v_c$, or $\sim 19\,\mathrm{km\,s^{-1}}$. This should show up as a $\cos 2\ell$ term in the Δv_{edge} curve (eq. 43) of amplitude $2\epsilon\alpha \sin\zeta$. A harmonic analysis of the observed curve gives a $\cos 2\ell$ term of at most $10\,\mathrm{km\,s^{-1}}$, consistent with the data as long as we are within $\sim 8°$ of a symmetry axis of the halo. However, a more detailed analysis, taking into account the quadrupole of the response of the disk to the halo potential, is required for a more thorough study of this model.

We now briefly discuss evidence for oscillations with $m \neq 2$. Many isolated disk galaxies exhibit large-scale asymmetries in their HI distributions outside the optical disk (Baldwin et al. 1980), which might be explained as large-amplitude $m = 1$ oscillations. Unfortunately, there are no convincing long-lived models of galaxies that exhibit these asymmetries, although the dominant instabilities in some galaxy models have $m = 1$ (Zang 1976, Toomre 1977, Zang and Hohl 1978, Sellwood 1985).

Axisymmetric ($m = 0$) oscillations can only be detected by detailed modelling of velocity fields. Thus they are likely to be difficult to detect. There is no strong theoretical reason to expect that axisymmetric oscillations are excited in disk galaxies; in fact, because the swing amplifier (Toomre 1981) amplifies only non-axisymmetric disturbances, it is likely that axisymmetric disturbances die away in a few galactic rotation periods. Nevertheless, we feel that fits of observations to models with all three wavenumbers $m = 2, 1, 0$ are important, to establish how well the observations discriminate between different models.

Summary

(i) We have examined the kinematics of the solar neighbourhood for evidence of oscillations. In a stationary, axisymmetric Galaxy, the following parameters should all be zero: the vertex deviation ℓ_v in the hot disk stars, the Oort constants C and K [or $\psi_v = -\frac{1}{2}\tan^{-1}(C/A)$], and the radial velocity of the LSR $v_{R,\mathrm{LSR}} = \overline{v_R}$. We estimate

$$\begin{aligned} \ell_v &= 5.5 \pm 4.2^\circ, \\ \psi_v &= -1.3 \pm 2.3^\circ, \\ K &= -0.35 \pm 0.5\,\mathrm{km\,s^{-1}\,kpc^{-1}}, \\ v_{R,\mathrm{LSR}} &= -1 \pm 9\,\mathrm{km\,s^{-1}}. \end{aligned} \tag{46}$$

All of these estimates are consistent with zero, as is the zero radial velocity of the Galactic centre HI absorption feature. Thus there is no strong evidence for large-scale oscillations from the kinematics of the solar neighbourhood.

(ii) The most comprehensive model of large-scale oscillations is that of Blitz and Spergel (1991a), who propose that the oscillations are induced by a rotating triaxial spheroid. In their model $m = 2$, $v_{R,\mathrm{LSR}} = 14\,\mathrm{km\,s^{-1}}$, the pattern speed is $\Omega_p = 5.5\,\mathrm{km\,s^{-1}\,kpc^{-1}}$, the inner Lindblad resonance is at $1.5R_\odot$, and the distant Galaxy is nearly axisymmetric. The principal evidence for their model is the asymmetry in the kinematics of the HI in the distant Galaxy. A possible problem is that there is no evidence of the strong velocity gradients that might be expected to be associated with the Lindblad resonance, either in stellar tracers outside the solar circle, or in the HI distribution at the anticentre. The B&S model also does not explain the asymmetry in the terminal velocity curves, although this may be due to spiral structure. The observations discussed in item (i) are reasonably consistent with the B&S model (which predicts $\ell_v = -9.3^\circ$, $\psi_v = -3.8^\circ$, $K = 0.4\,\mathrm{km\,s^{-1}\,kpc^{-1}}$, $v_{\mathrm{LSR}} = 14\,\mathrm{km\,s^{-1}}$) but are more consistent with axisymmetric, stationary models;

thus they do not provide evidence for the B&S model, although it is interesting that such a strong oscillation can be introduced without contradicting these null results.

(iii) An alternative model (Kuijken 1991) is that the Galaxy is approximately axisymmetric inside the solar radius but that an $m = 1$ ("lopsided") oscillation is present in the distant Galaxy. A possible problem is that asymmetries in the spatial density of HI suggest an $m = 2$ rather than $m = 1$ oscillation, although these are probably strongly affected by spiral structure near the solar circle. This model does not explain the asymmetry in the terminal velocity curves either. Lopsided models are less appealing because there is no strong theoretical reason to expect an $m = 1$ oscillation in the outer Galaxy; on the other hand they are observed!

(iv) The asymmetry in the shape of the Galactic warp cannot be removed by adjustments to kinematic distances, suggesting that the kinematics of the distant HI may not be described accurately by well-defined streamlines and a discrete oscillation spectrum. In this case there is no substantial evidence for any coherent large-scale oscillation of the Galaxy.

(v) If the Galactic halo is triaxial, the disk should exhibit an $m = 2$ oscillation with low pattern speed that increases in amplitude towards the outside of the Galaxy. There is no evidence for such an oscillation, though if the sun were near the major or minor axis of the halo such triaxiality would be extremely difficult to detect.

Acknowledgements. This research was supported by an operating grant from NSERC, by NSF grant AST-8913664, and by NASA grant NAGW-1448. ST thanks the California Institute of Technology for their hospitality and for the award of a Sherman Fairchild Scholarship. KK was supported in part by a Jeffrey L. Bishop Fellowship. We thank Leo Blitz, Ray Carlberg, Bruce Carney, Mike Fich, Alice Quillen, Allan Sandage, Paul Schechter, David Spergel, Peter te Lintel Hekkert, Alar Toomre, the Astronomical Data Center, and Martin Weinberg for discussions, data and advice.

References

Aaronson, M., Blanco, V. M., Cook, K. H., and Schechter, P. L. 1989. *Ap. J. Suppl.* **70**, 637.

Aaronson, M., Blanco, V. M., Cook, K. H., Olszewski, E. W., and Schechter, P. L. 1990. *Ap. J. Suppl.* **73**, 841.

Athanassoula, E., Bosma, A., Crézé, M., and Schwarz, M. P. 1982. *Astron. Astrophys.* **107**, 101.

Baldwin, J. E., Lynden-Bell, D. E. and Sancisi, R. 1980. *Mon. Not. Roy. Astron. Soc.* **193**, 313.

Bertola, F., Vietri, M. and Zeilinger, W. W. 1991. *Astrophys. J. Lett.* **374**, L13.

Binney, J. 1978. *Mon. Not. Roy. Astron. Soc.* **183**, 779.

Binney, J. 1987, in *The Galaxy*, eds. G. Gilmore and B. Carswell (Dordrecht: Reidel), 399.

Binney, J. and de Vaucouleurs, G. 1981. *Mon. Not. Roy. Astron. Soc.* **194**, 679.

Binney, J., Gerhard, O. E., Stark, A. A., Bally, J. and Uchida, K. I. 1991, preprint.

Binney, J. and Tremaine, S. 1987, *Galactic Dynamics* (Princeton: Princeton University Press).

Blitz, L., and Spergel, D. N. 1991a. *Astrophys. J.* **370**, 205. (B&S)
Blitz, L., and Spergel, D. N. 1991b, preprint.
Borderies, N., Goldreich, P., and Tremaine, S. 1983. *Icarus* **55**, 124.
Bosma, A. 1981. *Astron. J.* **86**, 1825.
Brand, J. 1986, *Ph.D. Thesis*, Leiden.
Burton, W. B. and Bania, T. M. 1974. *Astron. Astrophys.* **33**, 425.
Burton, W. B. and te Lintel Hekkert, P. 1986. *Astron. Astrophys.* **65**, 427.
Carney, B. W. and Latham, D. W. 1987. *Astron. J.* **92**, 116.
Chandrasekhar, S. 1942, *Principles of Stellar Dynamics*, (Chicago: University of Chicago Press).
Dekel, A. and Shlosman, I. 1983, in *Internal Kinematics and Dynamics of Galaxies*, IAU Symp. 100, ed. E. Athanassoula (Dordrecht: Reidel), 187.
Delhaye, J. 1965, in *Galactic Structure*, eds. A. Blaauw and M. Schmidt (Chicago: University of Chicago Press), 61.
Dubinski, J. and Carlberg, R.G. 1991, *Astrophys. J.*, in press.
du Mont, B. 1977. *Astron. Astrophys.* **61**, 127.
Eggen, O. J. 1965, in *Galactic Structure*, eds. A. Blaauw and M. Schmidt (Chicago: University of Chicago Press), 111.
Eggen, O. J. 1989. *Fund. Cosm. Phys* **13**, 1.
Erickson, R. R. 1975. *Astrophys. J.* **195**, 343.
Feast, M. W., Robertson, B. S. C., and Black, C. 1980. *Mon. Not. Roy. Astron. Soc.* **190**, 227.
Fich, M., Blitz, L. and Stark, A. A. 1989. *Astrophys. J.* **342**, 272.
Fich, M. and Tremaine, S. 1991. *Ann. Rev. Astron. Astrophys.* **29**, in press.
Fouts, G. and Sandage, A. 1986. *Astron. J.* **91**, 1189.
Freeman, K. C. 1970. *Astrophys. J.* **160**, 811.
Gliese, W. 1969, Veröff. Astr. Rechen-Inst., No. 22.
Godwin, P. J. and Lynden-Bell, D. 1987. *Mon. Not. Roy. Astron. Soc.* **229**, 7p.
Grosbol, P. J. 1985. *Astron. Astrophys. Suppl.* **60**, 261.
Güsten, R., Genzel, R., Wright, M. C. H., Jaffe, D. T., Stutzki, J., and Harris, A. I. 1987. *Astrophys. J.* **318**, 124.
Gwinn, C. R., Moran, J. M., Reid, M. J., Schneps, M. H., Genzel, R., and Downes, D. 1989, in *The Center of the Galaxy*, IAU Symp. 136, ed. M. Morris (Dordrecht: Kluwer), 47.
Hernquist, L. 1990. *Astrophys. J.* **356**, 359.
Hron, J. 1987. *Astron. Astrophys.* **176**, 34.
Humphreys, R. M. 1970. *Astron. J.* **75**, 602.
Jahreiss, H., and Wielen, R. 1983, in *The Nearby Stars and the Stellar Luminosity Function*, IAU Colloquium No. 76, eds. A. G. D. Philip and A. R. Upgren (Schenectady: L. Davis Press), 277.
Jaschek, C., and Valbousquet, A. 1991. *Astron. Astrophys.* **242**, 77.
Jenkins, A. and Binney, J. J. 1990. *Mon. Not. Roy. Astron. Soc.* **245**, 305.
Joy, A. H. 1939. *Astrophys. J.* **89**, 356.
Kent, S. M. 1990, in *Morphological and Physical Classification of Galaxies*, Proceedings of the OAC Fifth International Workshop, eds. G. Busarello, M. Capaccioli and G. Longo (Dordrecht: Kluwer), in press.
Kerr, F. J. 1962. *Mon. Not. Roy. Astron. Soc.* **123**, 327.
Kerr, F. J., and Lynden-Bell, D. 1986. *Mon. Not. Roy. Astron. Soc.* **221**, 1023.
Kinman, T. D., Feast, M. W., and Lasker, B. M. 1988. *Astron. J.* **95**, 804.
Kormendy, J. 1979. *Astrophys. J.* **227**, 714.
Kormendy, J. 1982, in *Morphology and Dynamics of Galaxies*, eds. L. Martinet and M. Mayor (Sauverny: Geneva Observatory), 113.
Kraft, R. P. and Schmidt, M. 1963. *Astrophys. J.* **137**, 249.
Kuijken, K. 1991, in *Warped Disks and Inclined Rings around Galaxies*, eds. S. Casertano, P. Sackett and F. Briggs, (Cambridge: Cambridge University Press), 159.

Lewis, B. M. 1987. *Ap. J. Suppl.* **63**, 515.
Lewis, J. R. 1990. *Mon. Not. Roy. Astron. Soc.* **244**, 247.
Lewis, J. R. and Freeman, K. C. 1989. *Astron. J.* **97**, 139.
Lindqvist, M., Winnberg, A., Habing, H. J., Matthews, H. E., and Olnon, F. M. 1989, in *The Center of the Galaxy*, IAU Symp. 136, ed. M. Morris (Dordrecht: Reidel), 503.
Liszt, H. S., and Burton, W. B. 1978. *Astrophys. J.* **226**, 790.
Liszt, H. S., and Burton, W. B. 1980. *Astrophys. J.* **236**, 779.
Lynga, G. and Palouš, J. 1987. *Astron. Astrophys.* **188**, 35.
Mayor, M. 1970. *Astron. Astrophys.* **6**, 60.
Mayor, M. 1972. *Astron. Astrophys.* **18**, 97.
McGinn, M. T., Sellgren, K., Becklin, E. E. and Hall, D. N. B. 1989. *Astrophys. J.* **338**, 824.
Milne, E. A. 1935. *Mon. Not. Roy. Astron. Soc.* **95**, 560.
Miralda-Escudé, J. and Schwarzschild, M. 1989. *Astrophys. J.* **339**, 752.
Murray, C. A., Argyle, R. W. and Corben, P. M. 1986. *Mon. Not. Roy. Astron. Soc.* **223**, 629.
Newton, A. J. 1986, D.Phil. thesis, Oxford University.
Oort, J. H. 1977. *Ann. Rev. Astron. Astrophys.* **15**, 295.
Radhakrishnan, V., and Sarma, N. V. G. 1980. *Astron. Astrophys.* **85**, 249.
Ratnatunga, K. A. and Upgren, A. R. 1991, *Astron. J.*, in press.
Reid, M. J. 1989, in *The Center of the Galaxy*, IAU Symp. 136, ed. M. Morris (Dordrecht: Kluwer), 37.
Rieke, G. H. and Rieke, M. J. 1988. *Astrophys. J. Lett.* **330**, L33.
Sellwood, J. 1985. *Mon. Not. Roy. Astron. Soc.* **217**, 127.
Sparke, L. S. and Casertano, S. 1988. *Mon. Not. Roy. Astron. Soc.* **234**, 873.
Staveley-Smith, L., Bland, J., Axon, D. J., Davies, R. D., and Sharples, R. M. 1990. *Astrophys. J.* **364**, 23.
Thomas, P. A. 1989. *Mon. Not. Roy. Astron. Soc.* **238**, 1319.
Toomre, A. 1977. *Ann. Rev. Astron. Astrophys.* **15**, 437.
Toomre, A. 1981, in *The Structure and Evolution of Normal Galaxies*, eds. S. M. Fall and D. Lynden-Bell (Cambridge: Cambridge University Press), 111.
Toomre, A. 1983, in *Internal Kinematics and Dynamics of Galaxies*, IAU Symp. 100, ed. E. Athanassoula (Dordrecht: Reidel), 177.
Tsioumis, A. and Fricke, W. 1979. *Astron. Astrophys.* **75**, 1.
van der Kruit, P. C., and Searle, L. 1982. *Astron. Astrophys.* **110**, 61.
Weinberg, M. 1991, preprint.
Wielen, R. 1974. *Highlights of Astronomy* **3**, 395.
Wielen, R. 1977. *Astron. Astrophys.* **60**, 263.
Wielen, R. 1979, in *The Large-Scale Characteristics of the Galaxy*, IAU Symp. 84, ed. W. B. Burton (Dordrecht: Reidel), 133.
Woolley, R. 1965, in *Galactic Structure*, eds. A. Blaauw and M. Schmidt (Chicago: University of Chicago Press), 85.
Zang, T. A. 1976, Ph.D. thesis, Massachusetts Institute of Technology.
Zang, T. A., and Hohl, F. 1978. *Astrophys. J.* **226**, 521.

Discussion

WHITE: There can be a serious difficulty in using apparent axis ratios to argue against circular disks in that small-scale "noise" (due to HII regions, spiral arms, etc.) always scatters the data toward higher apparent ellipticities. Are the analyses you referred to corrected for such effects?
TREMAINE: Kent obtains a distribution of apparent axis ratios that is uniform between 0.75 and 1 for a sample of nearly face-on galaxies, and corrects for noise and other selection effects to obtain an intrinsic axis ratio of 0.9. Errors due to spiral arms could be further reduced by using photometry in the near-infrared rather than in the visible.
NELSON: How does the bar of Blitz and Spergel and Weinberg compare with the HI bar observed at the galactic centre several years ago?
KUIJKEN: Blitz and Spergel (1991a, 1991b) actually detected two distinct $m = 2$ oscillations. One is a triaxiality of the extended Galactic "spheroid" or "thick disk", which would have to extend beyond the solar circle. The second oscillation, which appears to agree with the one detected by Weinberg (1991), affects the inner few kpc of the Galaxy only, and is unlikely to disturb the kinematics at the solar neighbourhood or beyond. This latter "bar" is in the same sense as the HI bar, and B&S even claim that it shares the tilt out of the Galactic plane that was proposed by Liszt and Burton (1980) for the much smaller molecular elliptical disk.
MERRIFIELD: If the vertex deviation of cold populations is caused by very local effects, whereas the vertex deviation of hotter populations is due to large-scale asymmetries in the Galaxy, is it just a coincidence that all populations seem to have a vertex deviation with the same sign?
TREMAINE: Yes.
GERHARD: Triaxial equilibrium models with $\rho \propto r^{-2}$ and small cores may not exist (Miralda-Escudé and Schwarzschild 1989), so the outer halo may not be able to sustain a triaxial shape.
BINNEY: We shouldn't forget that from ~ 10 kpc out there are clear indications that galaxies are not in anything like steady states. So one must trust with caution the argument that a configuration is improbable because no such equilibrium is possible.
KUIJKEN: I agree with Binney's comment. In any event, the Dubinski-Carlberg halos are obtained from an N-body integration and hence represent the dynamics self-consistently. The density of the Hernquist models that they approximate falls off more steeply than r^{-2} at large radii: the asymptotic decline is the same as for the so-called "perfect elliptical galaxies", which can be built self-consistently.
PFENNIGER: Do you assume that your elliptical deformation of a disk has a pattern speed? If not, it cannot be self-gravitating because loop orbits in a non-rotating potential are elongated perpendicularly to the potential.
TREMAINE: Our approximations take into account only the quadrupole from the (at most slowly-rotating) halo potential. It is true that the disk will tend to counteract this quadrupole moment somewhat.
BINNEY: Diego Garcia Lombas has recently analyzed a sub-sample of large galaxies in the APM survey. This sample is 5–10 times larger than that provided by the RC2 and much more homogeneous. He concludes that disk galaxies definitely cannot be modelled as axisymmetric systems. There is a deficit of apparently round systems, which requires disks to be elliptical.